Journal of Medicinal Chemistry

ARTICLE

pubs.acs.org/jmc

Azaxanthene Based Selective Glucocorticoid Receptor Modulators: Design, Synthesis, and Pharmacological Evaluation of (*S*)-4-(5-(1-((1,3,4-Thiadiazol-2-yl)amino)-2-methyl-1-oxopropan-2-yl)-5*H*-chromeno[2,3-*b*]pyridin-2-yl)-2-fluoro-*N*,*N*-dimethylbenzamide (BMS-776532) and Its Methylene Homologue (BMS-791826)†

David S. Weinstein,* Hua Gong, Arthur M. Doweyko, Mark Cunningham, Sium Habte, Jin Hong Wang, Deborah A. Holloway, Christine Burke, Ling Gao, Victor Guarino, Julie Carman, John E. Somerville, David Shuster, Luisa Salter-Cid, John H. Dodd, Steven G. Nadler, and Joel C. Barrish

Research and Development, Bristol-Myers Squibb Company, Princeton, New Jersey 08543-4000, United States

Supporting Information

ABSTRACT:

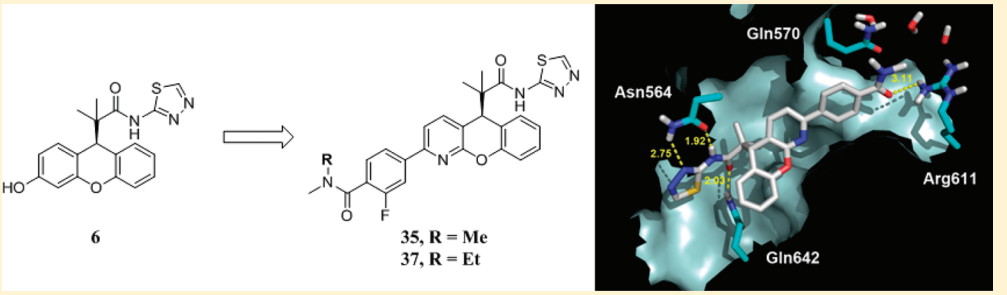

Structurally novel 5*H*-chromeno[2,3-*b*]pyridine (azaxanthene) selective glucocorticoid receptor (GR) modulators have been identified. A screening paradigm utilizing cellular assays of GR-mediated transrepression of proinflammatory transcription factors and transactivation of GR-dependent genes combined with three physiologically relevant assays of cytokine induction in human whole blood has allowed for the identification of high affinity, selective GR ligands that display a broad range of pharmacological profiles. Agonist efficacy in reporter assays can be tuned by halogenation of a pendent phenyl ring and correlates well with efficacy for cytokine inhibition in human whole blood. A hypothetical binding mode is proposed, invoking an expanded ligand binding pocket resembling that of arylpyrazole-bound GR structures. Two compounds of close structural similarity (**35** and **37**; BMS-776532 and BMS-791826, respectively) have been found to maintain distinct and consistent levels of partial agonist efficacy across several assays, displaying anti-inflammatory activity comparable to that of prednisolone **2** in suppressing cytokine production in whole blood and in rodent models of acute and chronic inflammation.

INTRODUCTION

Agonists of the glucocorticoid receptor (GR) have found broad utility in autoimmune and inflammatory diseases for over 60 years.[1] The unparalleled efficacy of these glucocorticoids (GCs), all of which are steroidal and are represented by dexamethasone (dex) **1**, prednisolone (pred) **2**, and deacylcortivazol (DAC) **3** (Chart 1), is countered by a host of side effects involving numerous organ systems, some of which can be debilitating (e.g., osteoporosis and diabetes).[2] GR (NR3C1) is a member of the nuclear receptor family of ligand-activated transcription factors. Its ubiquitous expression and central role in regulating the stress response and metabolic homeostasis are believed to underlie agonist-induced side effects. The search for selective modulators of GR has, for the most part, been predicated on a simplified view of receptor function: the ligand-activated GR provides anti-inflammatory efficacy through the transcriptional repression (transrepression, TR) of proinflammatory transcription factors such as AP-1 and NFkB, while side effects are induced through the transactivation (TA) of genes bearing GC response elements in their promoter regions. Ligands that modulate GR function in a pathway-selective manner ("dissociated agonists"), maintaining TR while minimizing TA, would be expected to maintain the clinical efficacy of traditional GR agonists while providing a relatively improved side effect profile.[3] Growing evidence suggests that ligands that completely dissociate these pathways may not be expected to meet this idealized clinical profile. For example, as various gene products

Received: July 5, 2011
Published: September 07, 2011

Chart 1

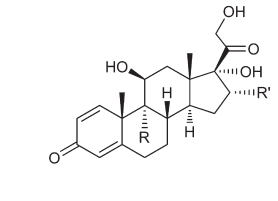

1 R = F, R' = Me, dexamethasone (dex)
2 R = H, R' = H, prednisolone (pred)

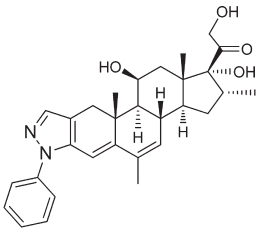

3 deacylcortivazol (DAC)

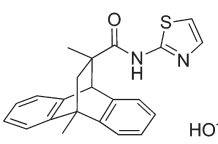

4

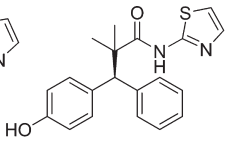

5

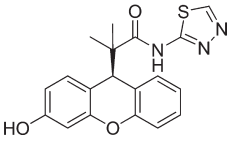

6

that are subject to GR-dependent TA contribute to the anti-inflammatory and immunosuppressive properties of GCs, complete dissociation may be expected to provide GR modulators of suboptimal efficacy in treating autoimmune disease.[4]

We recently described a series of diphenylpropionamides as agonists of the GR that maintain a dissociated pharmacological profile in cellular assays of TR and TA.[5,6] Ethano bridged 9,10-dihydroanthracenes (e.g., **4**) served as the starting point for these efforts, which, when substituted at the bridgehead position, provided in vitro profiles that would suggest a potential for anti-inflammatory efficacy with improved side effect profile relative to steroids.[5] We demonstrated in a subsequent report that several conformational constraints of this system were unnecessary for potent receptor binding, as uncyclized diphenylpropionamides (e.g., **5**) and xanthenes (e.g., **6**) maintained high GR binding affinity and agonist activity.[6] Notably, the in vitro dissociated profile of these phenolic ligands translated to potent in vivo efficacy in acute inflammation assays. Despite these promising advances, several problems remained to be

Table 1. 2-Phenylazaxanthene GR Agonists[a]

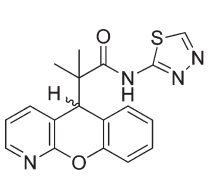

10

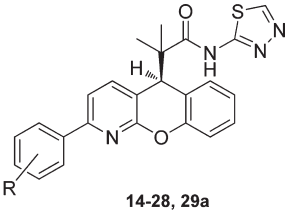

14-28, 29a

			AP-1 repression		E-selectin repression		GAL4 activation		TAT induction		GAL4 antagonist	
compd	R	GR binding K_i (nM)	EC_{50}, nM	% dex	EC_{50}, nM	% dex	EC_{50}, nM	% dex	EC_{50}, nM	% dex	EC_{50}, nM	max % inh
2		1.5	16.1	99	14.4	95	73.9	97	64	90	21	12
4		1.0	5.3	73	1.4	64	117	31				
5		1.2	40.9	63	29.5	52	372	21	251	21		
6		0.8	7.8	82	3.5	62	85.7	46	91.3	45		
10		412										
14	H	7.1	>1500				>10000		>5000	3	187	101
15	2-Me	10.5	122	41	>5000	14	>10000	1	>5000	11	1556	101
16	3-Me	24.0	654	32	>5000	14	>10000	1	>5000	13	1559	101
17	4-Me	2.5	46.8	70	26.6	49	2214	7	>5000	12	260	94
18	4-OMe[b]	49.5	>10000		355	21	>10000	0.6	>5000	2	4360	93
19	4-OMe	1.2	28.3	69	21.3	53	>10000	5	>5000	20	105	96
20	4-Et	1.0	17.7	87	8.3	70	108	56	732	44	27	49
21	4-^{n}Pr	2.4	15.1	87	29.7	67	126	44	823	49	36	58
22	4-O^{i}Pr	1.6	18.1	72			135	56	107	41	77	57
23	OH	5.7	90.8	91	108	44	>10000	3			201	96
24	NMe_2	3.8	13.6	86	20.0	38	926	13			242	87
25	4-SO_2Et	4.0	28.6	59	22.8	47	206	15	>5000	26	196	85
26	4-Ac	2.9	6.2	87	10.2	67	75.4	39	1097	55	31	72
27	3-F-4-O^{i}Pr	3.9	47.0	72	73	58	496	7	876	22	162	91
28	3-F-4-Ac	6.0	42	55			>10000	7	>5000	25	134	91
29a	4-CO_2H	15.4	544	75	1086	58	>10000	3			>5000	46

[a] Values represent the mean of at least two experiments. The standard deviation of the mean of GR K_i is <145%. AP-1 EC_{50} is <77%. AP-1 efficacy is <46%. E-selectin EC_{50} is <79%. E-selectin efficacy is <57%. GAL4 activation EC_{50} is <64%. GAL4 activation efficacy is <197%. TAT induction EC_{50} is <125%. TAT induction efficacy is <101%. GAL4 antagonist EC_{50} is <78%. GAL4 max % inh is <25%. [b] *R* isomer derived from intermediate **12b**.

dx.doi.org/10.1021/jm200879j |*J. Med. Chem.* 2011, 54, 7318–7333

Table 2. Benzamide GR Agonists[a]

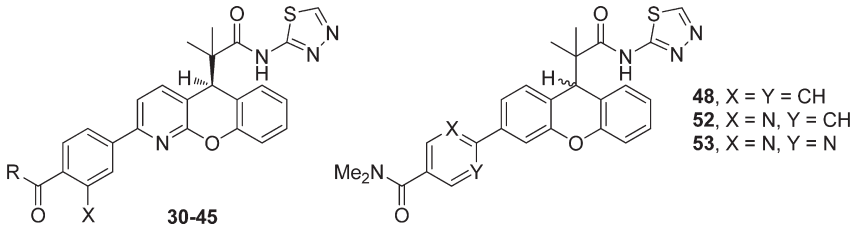

				AP-1 repression		E-selectin repression		GAL4 activation		TAT induction		GAL4 antagonist	
compd	R	X	GR binding K_i (nM)	EC_{50}, nM	% dex	EC_{50}, nM	% dex	EC_{50}, nM	% dex	EC_{50}, nM	% dex	EC_{50}, nM	max % inh
30	NH_2	H	2.50	>10000				>10000	1	>5000	19	201.5	100
31	NHMe	H	9.17	167	52	216	66	>10000	1	>5000	14	806.0	100
32	NHMe	F	5.48	34.1	38	157	26	>10000	0.3	>5000	20	408.0	102
33	NMe_2	H	1.74	12.2	85	4.6	75	89	58	22.7	67	42.7	46
34	NMe_2[b]	H	486	>10000				>10000	1	>5000	7	1740	104
35	NMe_2	F	1.94	33.2	70	33.8	63	242	32	150	39	142.7	68
36	NMeEt	H	0.67	17.4	86	7.8	78	32.4	76	740	91	36.7	33
37	NMeEt	F	1.64	17.7	79	6.89	77	98.5	57	88	57	113.4	53
38	NMeEt	Cl	15.7	124	76	64.9	77	702	46	2403	45	721.1	68
39	piperidine	H	1.3	15.7	65	28.6	52	273	24	>5000	25	167.1	76
40	piperidine	F	1.68	27.5	48	25.6	55	>10000	8	>5000	19	203.6	94
41	morpholine	H	2.60	12.4	89	6.3	75	39.2	70			28.6	21
42	morpholine	F	2.70	11.7	79	11.7	80	78.9	62	93	75	34.4	40
43	pyrrolidine	F	1.96	25.0	77	29.2	75	177	39	389	40	205	74
44	3,3-difluoropyrrolidine	F	2.53	37.9	79	20.6	77	192	43	1989	46	99.3	57
45	3,3-difluoropyrrolidine	Cl	3.08	50.0	90	33.8	68	165	44	329	49	129.7	56
48			8.60	77.9	65	74.9	49	>10000	11	>5000	24	610	89
52			4.1	58.0	63			382	23	>5000	29	162	75
53			4.2	183	85			596	26			592	76

[a] Values represent the mean of at least two experiments. The standard deviation of the mean of GR K_i is <81%. AP-1 EC_{50} is <88%. AP-1 efficacy is <42. E-selectin EC_{50} is <113%. E-selectin efficacy is <14%. GAL4 activation EC_{50} is <72%. GAL4 activation efficacy is <34%. TAT induction EC_{50} is <137%. TAT induction efficacy is <72%. GAL4 antagonist EC_{50} is <86%. GAL4 max % inh is <27%. [b] *R* isomer derived from intermediate **12b**.

addressed with this series. Phenols **5** and **6** maintained only modest selectivity for GR over the progesterone receptor (PR), a reflection of both the phylogenetic similarity of these two nuclear receptors and the in silico screening methodology (virtual screen utilizing a PR-based homology model of GR) from which the initial 9,10-dihydroanthracene leads were first identified.[5] Significant concern also arose out of the likelihood of oxidation of the phenol to a 1,4-quinone methide. Similar metabolic activation of phenols bearing alkyl groups at the para position and the associated toxicity of resulting 1,4-quinone methides have been well documented.[7] Efforts were undertaken to identify a GR pharmacophore that would preclude the liabilities associated with these phenols while maintaining their promising pharmacological profiles.

It was previously surmised that the phenolic hydroxyl groups of **5** and **6**, modeled to interact with the Arg611 and Gln570 residues of helices 5 and 3, respectively, triggered agonist activity by mimicking the C-3 carbonyl oxygen of steroids such as **1** and **2**. Efforts were undertaken to identify replacements for this functionality that would preclude metabolic activation and potential toxicophore generation. Other potential hydrogen bond acceptors or donors that could be expected to engage the adjacent Arg611/Gln570 residue pair in the ligand binding pocket were evaluated as phenol replacements, but useful agonist activity was not uncovered through those efforts (unpublished results). The introduction of a pyridine nitrogen to the xanthene core of **6** provided a useful synthetic handle for functionalization, and arylation adjacent to the pyridine nitrogen provided ligands with a broad range of pharmacology (Tables 1 and 2). Structure–activity relationships for tuning agonist activity were uncovered, leading to the identification of two potent and selective ligands (**35** and **37**; BMS-776532 and BMS-791826, respectively) with overall in vitro biological profiles that are clearly distinct from those of steroidal glucocorticoids and from each other. The pharmacological properties of these ligands as described herein show promise for maintaining the anti-inflammatory properties of traditional steroid agonists **1**–**3** with an improved clinical side effect profile.

CHEMISTRY

A series of 2-aryl-5*H*-chromeno[2,3-*b*]pyridines (azaxanthenes) was prepared efficiently as shown in Scheme 1. Reduction of 1-azaxanthone **7** provided the secondary alcohol **8**. Installation of

dx.doi.org/10.1021/jm200879j |*J. Med. Chem.* 2011, 54, 7318–7333

Scheme 1[a]

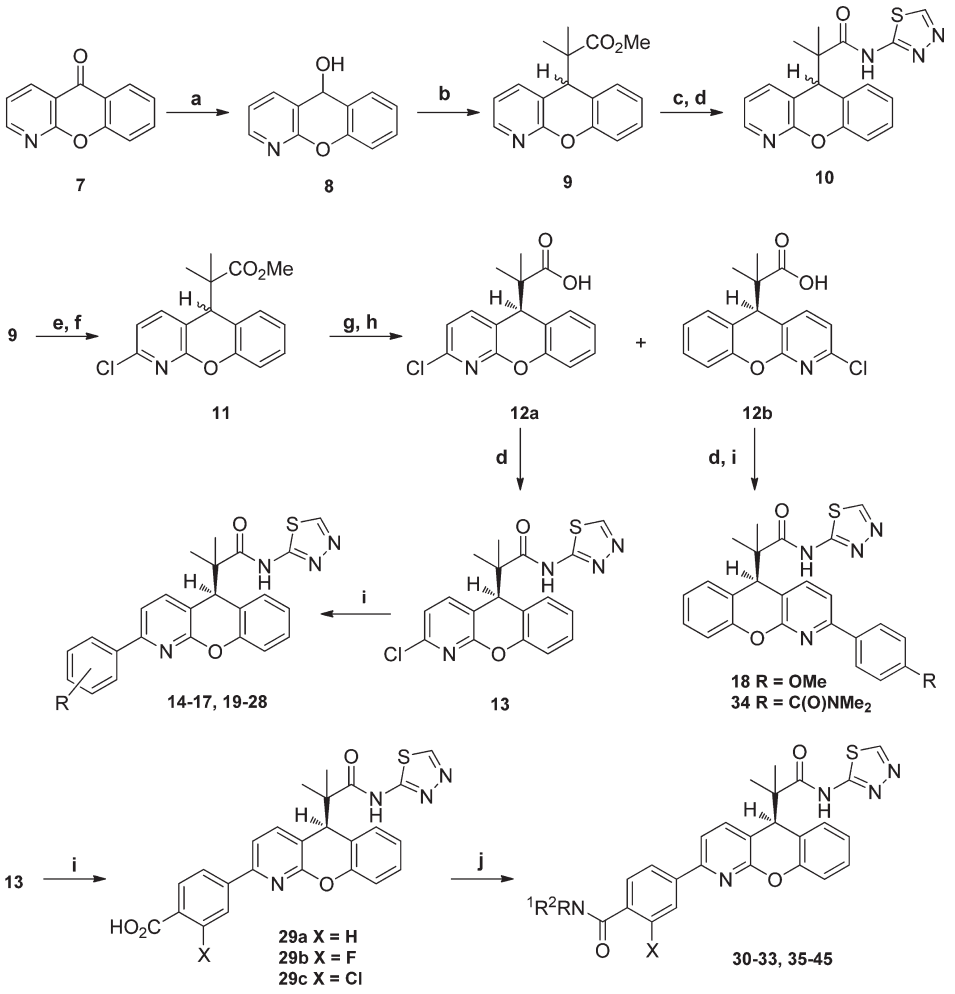

[a] Reagents and conditions: (a) $NaBH_4$, MeOH, 0 °C, then room temp, 95%; (b) $TiCl_4$, $(CH_3)_2C{=}C(OCH_3)OSiMe_3$ THF, 0 °C, then room temp, 89%; (c) 40% aq KOH, THF, MeOH, 65 °C, 90%; (d) 1,3,4-thiadiazol-2-amine, HATU, Et_3N, CH_3CN, 80 °C, 12 h, 79−83%; (e) mCPBA, CH_2Cl_2, room temp, 2 h, 97%; (f) $POCl_3$ (neat), 90 °C, 30 min, 77%; (g) 40% aq KOH, THF, MeOH, 65 °C, 90%; (h) SFC chiral separation with various chiral columns using CO_2/MeOH as mobile phase; (i) boronic acid, $Pd(PPh_3)_4$, K_3PO_4 (2 M solution in water), DMF, 100 °C, 5 h, 75−85%; (j) amine, HOBT hydrate, EDC, CH_3CN, $^iPr_2NEt$, room temp, 12 h. 70−81%.

the isobutyrate fragment was readily achieved by treatment of the highly electrophilic, doubly benzylic alcohol **8** with the silyl ketene acetal of methyl isobutyrate under Lewis acid promoted (Mukaiyama) conditions to provide methyl ester **9** as a racemic mixture. Saponification of the methyl ester followed by condensation with 2-aminothiazole provided amide **10**. Treatment of pyridine **9** with mCPBA followed by exposure to phosphorus oxychloride effected a regioselective chlorination to provide chloroazaxanthene **11**. Saponification of methyl ester **11** gave a racemic mixture of carboxylic acids in high yield, which were readily separated by chiral supercritical fluid chromatography (SFC) to provide the homochiral enantiomeric acids **12a** and **12b**. An X-ray crystal structure of the (*R*)-(+)-α-methylbenzylamine salt of **12b** revealed it to be of the *R* absolute configuration. Condensation with 2-amino-1,3,4-thiadiazole and subsequent Suzuki−Miyaura coupling of chlorides **12a** and **12b** with various arylboronic acids provided 2-aryl-5*H*-chromeno[2,3-*b*]pyridines **14**−**28**, **29a**−**c**, and **34**. Benzamides **30**−**33** and **35**−**45** were readily prepared by condensation of **29a**, **29b**, or **29c** with various amines.

To evaluate the role of the azaxanthene nitrogen, several aryldimethylcarboxamide-containing xanthenes were also prepared in a straightforward manner from racemic hydroxyxanthene **46** (Scheme 2). Conversion to its triflate **47** followed by Suzuki coupling with 4-[*N*,*N*-dimethylaminocarbonyl]phenylboronic acid provided the benzamide xanthene **48**. Alternatively, Miyaura borylation of triflate **47** provided pinacol boronate **49** in good yield. Arylation of boronate **49** with the appropriate carboxylic acid containing aryl halides provided the nicotinic acid **50** and pyrimidine acid **51**. Subsequent condensation with dimethyl amine provided the corresponding dimethylamides **52** and **53**.

RESULTS AND DISCUSSION

The in vitro assays used to characterize biological activities of the GR ligands including nuclear receptor binding, transrepression [AP-1 and E-selectin (NFκB dependent)], and transactivation in GAL4-reporter and tyrosine amino transferase (TAT) assays have been previously reported.[6] To further characterize

dx.doi.org/10.1021/jm200879j |*J. Med. Chem.* 2011, 54, 7318–7333

Scheme 2[a]

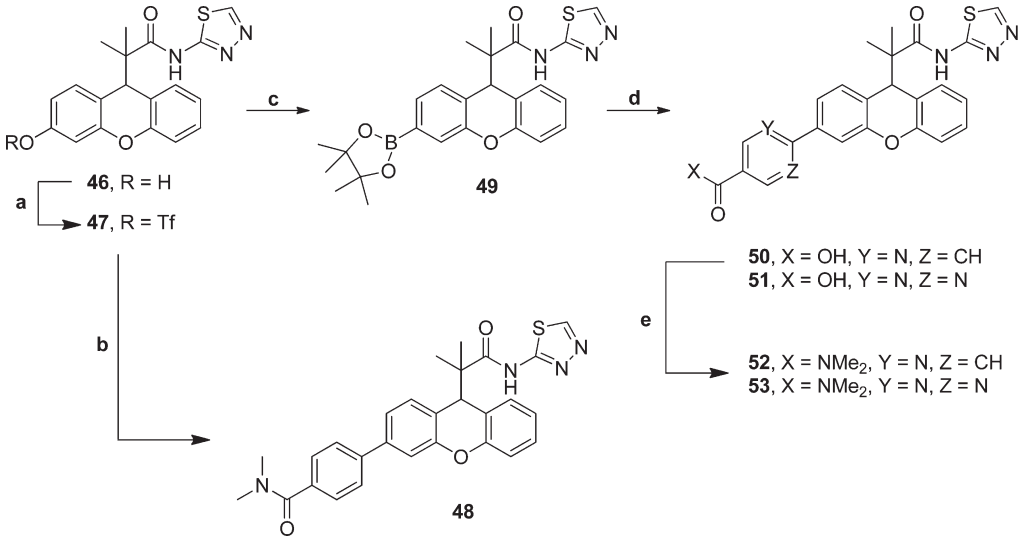

[a] Reagents and conditions: (a) $PhNTf_2$, Et_3N, CH_2Cl_2, 0 °C, 2.5 h, 55%; (b) $Pd(PPh_3)_4$, 4-[*N*,*N*-dimethylaminocarbonyl]phenylboronic acid, K_3PO_4, DMF, 120 °C, 0.5 h, 30%; (c) $PdCl_2$(dppf), bis(pinacolato)diboron, KOAc, dioxane, 80 °C, 5 h, 79%; (d) $Pd(PPh_3)_4$, 6-chloronicotinic acid or 2-bromopyrimidine-5-carboxylic acid, K_3PO_4, DMF, 100 °C, 2 h, 20−30%; (e) HOBt, EDCI, dimethylamine, Et_3N, CH_3CN, 80 °C, 12 h, 35−55%.

Table 3. Human Whole Blood Cytokine Inhibitory Activity of Selected Agonists[a]

	LPS-induced TNFα		TNFα-induced IL-8		IL-1β-induced IL-8	
compd	EC_{50}, nM	% dex	EC_{50}, nM	% dex	EC_{50}, nM	% dex
dex, **1**	6.9	100	6.4	100	5.1	100
pred, **2**	89	94	124	94	104	94
27	>5000	49	>20000	12	>20000	7
32	819	58	>20000	15	>20000	35
35	830	83	1469	55	1136	70
36	78.5	100				
37	379	91	532	76	628	88
40	5474	73	>20000	45	3193	27
42	469	88	382	84	789	92
43	886	80	1295	61	238	86
44	4019	78	3068	67	2493	81
45	932	85	2851	59	5248	82

[a] Values represent the mean of at least two experiments. The standard deviation of the mean of GR LPS-induced TNF EC_{50} is <85%. LPS-induced TNF efficacy is <23%. TNF-induced IL-8 EC_{50} is <109%. TNF-induced IL-8 efficacy is <54%. IL-1 induced IL-8 EC_{50} is <197%. IL-1 induced IL-8 efficacy is <21%.

Table 4. Alkaline Phosphatase and Glutamine Synthetase Induction by 2, 35, and 37

		hGS induction	
	AlkPhos[a]		
compd	% max induction ± SD (*n*)	EC_{50} ± SD, nM (*n*)	% pred ± SD
pred, **2**	68 ± 16 (31)	19 ± 11 (25)	100 ± 17
35	13 ± 13 (12)	44 ± 22 (22)	33 ± 11
37	24 ± 12 (10)	207 ± 22 (23)	53 ± 15

[a] Induction measured after 3 days of incubation at 600 nM.

Table 5. Nuclear Hormone Receptor Selectivity[a]

compd	pred	**5**	**6**	**21**	**22**	**33**	**35**	**37**
GR K_i, nM	1.5	1.2	0.8	2.4	1.6	1.7	1.9	1.6
PR K_i, nM	>6000	273	53	285	310	1228	1529	1829
AR K_i, nM		1058	696	>5000			>5000	>5000
ERα K_i, μM	>5	>100	5.5			>75	>75	>75
MR agonist[b]	0.002(88)	>5	>5			>5	>5	>5

[a] Values represent the mean of at least two experiments. [b] In A549 cell line, EC_{50} (μM)/(% maximal efficacy) determination (aldosterone as a positive control).

functional activity of agonists and partial agonists in the GAL4 assay, compounds were also evaluated for their ability to antagonize glucocorticoid response element (GRE) activation induced by **1**. While some level of TA may likely be required for anti-inflammatory efficacy paralleling that of steroidal full GR agonists (vide supra), it is also well established that TA of specific genes contributes to the toxicity of glucocorticoids. In order to rapidly identify the minimal TA requirement for anti-inflammatory efficacy in vivo, compounds were first studied in three moderate throughput, highly physiologically relevant assays of cytokine production in human whole blood. This panel of assays involved measuring the ability of compounds to inhibit production of tumor necrosis factor α (TNFα) induced by lipopolysccharide (LPS) or interleukin-8 (IL-8) induced by TNFα or interleukin-1 (IL-1β) in freshly drawn human whole blood. Data are provided in Tables 1−5.

The relatively weak GR binding affinity of compound **10** (GR K_i = 412 nM) was improved with the incorporation of substituents adjacent to the pyridine nitrogen of the azaxanthene core (Table 1). The unsubstituted phenyl substituent of **14** increased binding affinity more than 10-fold relative to **10**. While being a

high affinity ligand, **14** lacked agonist activity in transrepression (AP-1) and transactivation (GAL4 and TAT induction) assays. Compound **14** did, however, potently antagonize the activity of **1** (100 nM) in the GAL4 assay. The effects of various substituents appended to the azaxanthene C-2 phenyl ring were studied (Table 1). A single methyl group was transposed around the pendent phenyl group of the *S* enantiomer of the azaxanthene. The ortho and meta isomers (**15** and **16**, respectively) provided only weak activity in the AP-1 assay while being inactive in the E-selectin and GAL4 assays. Para isomer **17**, however, proved to be a higher affinity ligand (GR K_i = 2.5 nM) than both isomers **15** and **16**, just 2- to 3-fold less potent than **2** in both assays of TR and inactive in both assays of TA. The promising profile of **17** warranted further SAR exploration around the para substituent of the phenylazaxanthenes. The same stereochemical preference as previously reported for hydroxyxanthene **6** was observed.[6] Thus, a methoxy group in the context of the *S* enantiomer provided binding potency equivalent to that of **2** (**19**, GR K_i = 1.2 nM), while *R* enantiomer **18** was 50-fold less potent (GR K_i = 49.5 nM). Like *p*-methyl compound **17**, *p*-methoxy compound **19** displayed an interesting partial agonist profile in the transrepression assays while nearly fully antagonizing GRE activation in the transactivation assays. Increasing the size and bulk of the para substituent led to marked increases in potency and efficacy in agonism of both transrepression and transactivation. A single carbon extension of *p*-methyl **17** to *p*-ethyl **20** led to a 17−21% increase in efficacy in AP-1 and E-selectin TR assays, respectively, and a more significant 49% increase in efficacy and 20-fold increase in potency for TA in the GAL4 assay. The *n*-propyl compound **21** maintained a similar level of agonist activity as ethyl compound **20**. While the 4-isopropoxy compound **22** provided AP-1 TR similar to 4-methoxy compound **19**, the two diverge in their TA profiles, with compound **22** proving to be a partial agonist of TA in both the GAL4 and TAT induction assays (56% and 41% E_{max}, respectively) unlike the antagonist profile of compound **19**. The phenol **23** displayed an overall profile similar to that of methoxy compound **19** (i.e., partial agonism of TR with potent, full antagonism of TA), while the dimethylaniline **24**, ethylsulfone **25**, and methyl ketone **26** displayed partial agonism of both TR and TA. Introduction of a 3-fluoro substituent to isopropoxy compound **22** or acetophenone **26** (ligands **27** and **28**, respectively) significantly attenuated TA efficacy in both cases. Overall, the partial agonist profiles of **19**−**22** and **26** for TR and TA were found to resemble those of the phenol progenitors, compounds **5** and **6**.

While the benzoic acid **29a** was a weak partial agonist in the AP-1 and E-selectin assays, related benzamides were found to be potent, partial agonists of TR with a broad range of activities in TA (Table 2). The primary amide **30**, although a high affinity ligand, was inactive in the AP-1 assay. The secondary methylamide **31** was found to be a weak partial agonist in the TR assays. With regard to transactivation, both primary amide **30** and methylamide **31** were inactive as agonists of TA and were fully efficacious in the GAL4 assay in antagonist mode. Tertiary amides, however, were found to be potent partial agonists. The dimethylamide **33** provided potency comparable to that of **2** in TR and TA assays (EC_{50} of 12.2 nM in AP-1, 4.6 nM in E-selectin, 89 nM in GAL4 and 23 nM in TAT). While the agonist efficacy of dimethylamide **33** in both assays of TR was only marginally diminished relative to **2**, it was >30% less efficacious in both TA assays. Consistent with the stereochemical preference of non-benzamide-containing compounds (i.e., **18** vs **19**), the enantiomer of **33** (*R* isomer **34**) was determined to be a very weak GR ligand (GR K_i = 486 nM). As noted with the two pairs of nonhalogenated and meta-fluorinated compounds (isopropoxy compounds **22** and **27** and methyl ketones **26** and **28**), a meta-halogenated para-benzamides were consistently at least 10% less efficacious in assays of TA than nonhalogenated comparators. This effect was pronounced in the case of *m*-fluoro dimethylamide **35**, which was nearly 30% less efficacious in both TA assays relative to its nonhalogenated comparator **33**. Similarly, both *m*-fluoro and *m*-chloro ethylmethylamides (**37** and **38**, respectively) were significantly less efficacious in both TA assays than **36**, with chloro analogue **38** being significantly less potent than **36** or **37**. This trend was found to continue with piperidine amides (**39** and **40**) and morpholine amides (**41** and **42**). The pair of secondary benzamides **31** and **32** followed this trend in efficacy (with fluorinated **32** being less efficacious than **31** in TR assays), albeit with somewhat more potency for the less efficacious of the two.

It is interesting to note the complementary activities for this class of ligands in the agonist and antagonist modes of the GAL4 transactivation assay; the sum of efficacy for any given ligand in agonist mode and the maximal inhibition it provided in antagonist mode was invariably found to be close to 100%. The observed linear relationship between efficacy in the agonist and antagonist mode of the GAL4 assay is consistent with competitive partial agonism/partial antagonism of transactivation by the azaxanthene ligands. Thus, while these ligands effectively compete with **1** for receptor binding, the maximum level of functional antagonism they provide is limited to the extent these competing ligands likely induce a receptor conformation consistent with agonism, albeit not as effectively as **1**. In addition to replacing a phenolic hydroxy group with aryl substituents, the replacement of a carbon of the xanthene core of **6** with a pyridine nitrogen in the case of the present azaxanthenes represents another perturbation, the effect of which was of interest for evaluation. To this end, several compounds that maintain the dimethylamide of **33** but in the context of the xanthene system were evaluated (**48**, **52**, **53**). The phenyl-, 2-pyridyl-, and 2-pymidinylxanthenes were found to retain the high GR binding affinity of **33** and its congeners. However, the pharmacological profile of all three more closely represents methylamide **31** or fluorinated piperidine amide **39** than the tertiary benzamides represented by **33**. Specifically, the xanthenes **48**, **52**, and **53** retained moderate agonism of TR while being very weak partial agonists of TA. The significant difference in levels of agonism achieved by the xanthene amides **48**, **52**, and **53** versus azaxanthene **33** is not readily explained by differences in any particular ligand/protein interactions (vide infra) but may be a reflection of small differences in conformational preferences of the ligands, possibly with respect to rotational preferences around the bond between the tricyclic core and pendent aryl ring. These differences may provide differential effects on receptor dynamics, coactivator recruitment, and overall pharmacology.

A structural model has been utilized to rationalize the GR binding and agonist activity of this class of ligands. Docking of ligand **33** into the published crystal structure of **1** bound to the GR ligand binding domain[8] revealed steric and electronic clashes with the portion of the ligand binding pocket in the vicinity of the Arg611 and Gln 570 pair, a problem not encountered previously when the less sterically demanding phenols **5** and **6** were docked into this structure.[6] The reported crystal structure of **3** bound to GR (3BQD.pdb) revealed a significant repositioning of these

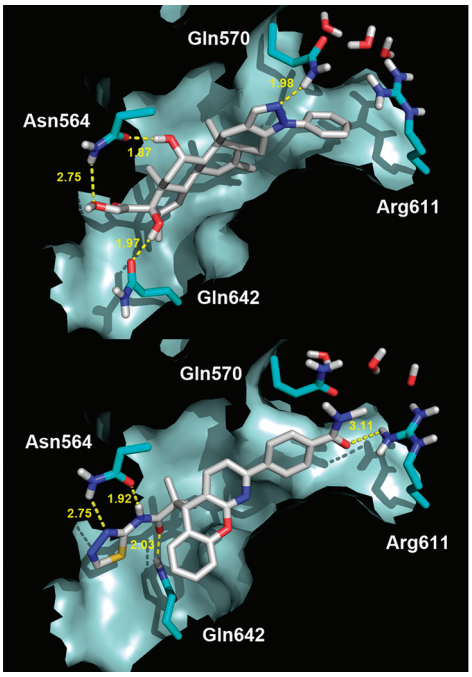

Figure 1. (Top) Deacylcortivazol **3** (3BQD) structure illustrating the major H-bonding contact residues and three water molecules in the expanded ligand binding pocket (in the vicinity of Arg611/Gln570). Hydrogens were added and allowed to assume optimal orientations. H-bonding distances (in angstroms) are noted between the ligand and Gln642, Asn564, and Gln570. (Bottom) Ligand **33** modeled into the 3BQD structure. Hydrogens were added, and contact residues and three water molecules in the Gln570/Arg611 region were allowed to relax using the Amber force field as implemented within Flo (Thistlesoft, Colebrook, CT).

residues relative to the dexamethasone-bound structure, with an effective doubling of the volume of the ligand binding pocket (Figure 1).[9] We reasoned that a similar rearrangement could accommodate azaxanthenes with para-substituted aryl substituents, and docked representative ligand **33** into the 3BQD structure accordingly. When contact residues were allowed to relax in place, the ligand binding pocket was found to remain similar to that of the 3BQD structure, in terms of both the van der Waals surface and its overall size and shape. As suggested in previous models of diarylpropanamide GR ligands, a triad of H-bonds between the thiadiazole amide moiety of the ligand, Asn564, and Gln642 is invoked, mirroring interactions of these residues and C-11 β-hydroxyl and D-ring C-17 substituents of steroidal ligands, respectively. A significant repositioning of Gln642 allows an H-bond to the propanamide carbonyl oxygen. Of the many possible orientations of the Arg611/Gln570·$3H_2O$ system, it was found that a small perturbation of Arg611 allows interaction with the benzamide portion of the ligand with only minor changes to the water molecule positions. A similar structure-based rationale invoking the expanded ligand binding pocket of the 3BQD structure was reported in the design of a series of meta-substituted phenylindazoles and ultimately validated with the solution of crystal structures of two representative ligands bound to the GR ligand binding domain.[10] The meta substituents were found to occupy a channel ("meta channel") accessible to ligands in the expanded 3BQD but not the **1**/GR crystal structure. The significant differences in pharmacology accompanied by only minor differences within the azaxanthene class of ligands, especially involving the substituents on the pendent aryl ring, are not readily explainable with the binding model alone. However, the para-substituted benzamide portion of this class of ligands protrudes into the previously identified "meta channel". It has been noted that perturbation of the homologous region of the estrogen receptor (ERα), through binding of a peptide ligand or residue mutation, leads to altered TIF-2 binding despite its remoteness from the coactivator binding (AF-2) site.[11] The effects of azaxanthene ligand binding on GR coactivator recruitment will be reported at a later date.

The clinical efficacy of glucocorticoids has been ascribed in large part to their ability to inhibit the downstream production of proinflammatory cytokines.[12] Ligands representing a wide range of profiles in the TR and TA assays were thus evaluated for their ability to inhibit the production of proinflammatory cytokines in human whole blood after various stimuli (Table 3). **1** was found to potently inhibit the production of TNFα in response to LPS, and IL-8 production in response to either TNFα or IL-1β stimuli, with nearly complete inhibition at saturating concentrations. **2** provided similar efficacy in all three assays, with somewhat lower potency, consistent with results in the cellular reporter assays. Compounds that demonstrated only weak activity in the TR assays, with little or no activity in the assays of TA (**27**, **32**, and **40**), did not inhibit IL-8 production in human whole blood in response to either TNFα or IL-1β. Notably, these compounds were able to achieve partial efficacy in inhibiting the production of TNFα in response to LPS. Partial agonists of TR and TA (**35**, **37**, **42**−**45**) gave particularly promising cytokine inhibition profiles; these ligands potently inhibited production of both cytokines in all three whole blood assays, with efficacy approaching that of steroid agonists in inhibiting LPS-induced TNFα and IL-1β-induced IL-8 and with somewhat lower efficacy in inhibiting TNFα-induced IL-8. Notably, the whole blood potency recorded for partial agonists is closer to that recorded in the GAL4 activation than transrepression assays. This observation is consistent with a requirement for transactivation of anti-inflammatory gene products to inhibit cytokine production in human primary cells and the lack of whole blood potency recorded in IL-8 assays for ligands lacking GAL4 agonist activity. Dimethylamide **35** and methylethylamide **37** were of particular interest for further exploration. Ligand **35** represented a lower limit in TA activity while still providing promising activity in the cytokine assays and would be expected to provide a uniquely differentiated profile from steroids in follow-up studies. Ligand **37**, with its consistently higher efficacy compared with **35** in assays of TR and TA and roughly 2-fold higher potency in whole blood cytokine assays, would be an interesting comparator, particularly given its very close structural similarity to **35** and likelihood for similar ADME profile in vivo.

To further explore the potential for an improved side effect profile relative to steroids in humans, both **35** and **37** were evaluated in cellular assays of gene products known to be induced by glucocorticoids in osteoblastic cells, bone-specific alkaline phosphatase (ALP), and glutamine synthetase (GS).[13,14] In the SAOS-2 osteosarcoma cell line, **2** was found to induce ALP (68% above background) after a 3-day incubation (Table 4). As in the TA reporter assays, **35** and **37** were significantly less efficacious than **2**. The rank order for efficacy was consistent with that observed in the reporter assays, with **35** being significantly less efficacious than **37** (13% and 24% maximal induction, respectively). Similarly, in the MG-63 osteosarcoma cell line, less

Table 6. Rat Pharmacokinetic Properties of 35 and 37

compd/route/dose	C_{max} (ng/mL)	T_{max} (h)	AUC (ng·h/mL)	$T_{1/2}$ (h)	Cl (mL min^{-1} kg^{-1})	V_{ss} (L/kg)	F (%)
35/iv/1 mg/kg			342	0.6	49.5	1.0	
35/po/10 mg/kg	285	1.3	673				20
35/po/50 mg/kg	3209	1.7	20186				119
37/iv/1 mg/kg			526	0.4	34.0	0.5	
37/po/10 mg/kg	351	1.0	904				17
37/po/50 mg/kg	3083	3.3	28122				107

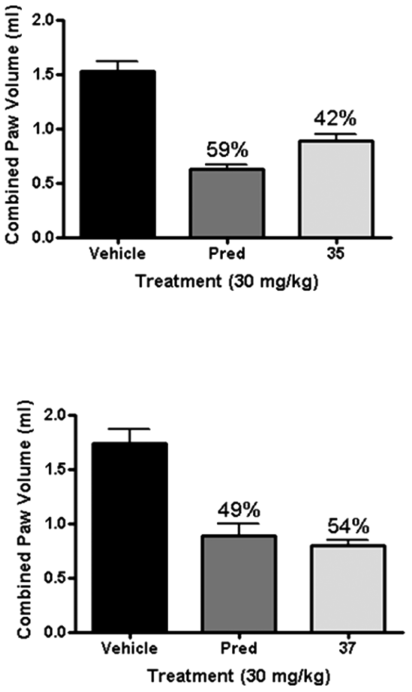

Figure 2. Compounds **35** (top), **37** (bottom), and **2** in the carrageenan-induced paw edema model after oral administration in rats (30 mg/kg). Paw edema was measured 6 h postdose.

efficacy than **2** for induction of GS was observed for **35** and **37** (33% and 53% of **2**), with a similar level of potency.

The selectivity of GR ligands over closely related nuclear receptors is of paramount importance for their safety and successful clinical development. At least some of the adverse cardiovascular effects of traditional steroidal GR ligands have been attributed to their potent agonism of the mineralocorticoid receptor (MR).[15] We previously reported that diarylpropanamide phenols **5** and **6** are highly selective over the MR as well as androgen and estrogen receptors (AR, ERα). Some affinity for the progesterone receptor (PR) remained a concern. Xanthene **6**, for example, is a relatively potent ligand of the PR (K_i = 53 nM). Subsequently, compound **6** was found to be a potent (EC_{50} = 77 nM) and efficacious (97% of progesterone efficacy) agonist in a cellular reporter assay of PR transactivation. Azaxanthenes with various substituents at the para position of the pendent phenyl ring were generally found to be at least several-fold more selective over the PR than phenol **6** and at least as selective as phenol **5**. Carboxamides at the para position provided even more selectivity than other substituents, as exemplified by amides **33**, **35**, and **37** (all of which bound PR with K_i > 1000 nM).

In Vivo Evaluation. The pharmacokinetic properties of **35** and **37** were evaluated in male Sprague−Dawley rats, and similar properties were noted for both compounds (Table 6). Despite moderate to high systemic plasma clearance after a single intravenous dose of either compound, promising exposures were noted after oral dosing. The oral bioavailability of both compounds is consistent with high intestinal absorption and agrees well with generally high passive transcellular permeability as measured in the parallel artificial membrane permeability assay (PAMPA) for this series of compounds (data not shown). Oral exposures (both C_{max} and AUC) were found to increase more than dose-proportionally for both compounds, with a 50 mg/kg dose providing complete (100%) oral bioavailability. In order to estimate the systemic exposures that might be required for efficacy after oral administration in a rodent inflammation model, both compounds were evaluated first for their ability to inhibit the production of LPS-induced TNFα in whole blood from rats. Potency was found to be comparable to that measured in human blood (EC_{50} of 189 nM for **35** and 215 nM for **37**), with both compounds inhibiting >95% of TNFα production at the highest concentrations.

Compounds **35** and **37** were first evaluated for anti-inflammatory efficacy in the rat carrageenan-induced paw edema (CPE) model. An acute inflammatory response was generated in Sprague−Dawley rats (n = 8/group) by injecting both hind paws with carrageenan 2 h after a single 30 mg/kg oral dose of **35**, **37**, or **2**, and paw volumes were measured 4 h after the carrageenan challenge (Figure 2). Paw swelling was calculated by subtracting the baseline values from the postchallenge measurements. Compounds **35** and **37** both proved to be efficacious, providing paw volumes representing 42% and 54% of the vehicle control (p < 0.01), respectively, comparing well with the efficacy of **2** (49−59% of control, p < 0.01). The plasma exposures of both compounds were also measured 6 h postdose and were determined to be several-fold higher than their respective potencies for inhibiting LPS-induced TNFα in rat whole blood. Thus, **35** provided 788 nM exposure at 6 h (4.2-fold above IC_{50}) while **37** provided 1114 nM exposure (5.2-fold above IC_{50}).

The anti-inflammatory efficacy of compounds **35** and **37** were also evaluated in a dose response study in the chronic model of adjuvant-induced arthritis (Figure 3). Male Lewis rats were first inoculated with *Mycobacterium butyricum* in incomplete Freund's adjuvant, and both compounds were dosed preventatively from day 0 to day 21. A dose-dependent reduction in the onset and progression of arthritis was observed for both compounds. Both compounds achieved efficacy equivalent to that from daily 5 mg/kg oral doses of **2** (**35**, 50 mg/kg; **37**, 25 mg/kg). ED_{50} values of approximately 17 and 8 mg/kg were determined for compounds **35** and **37**, respectively.

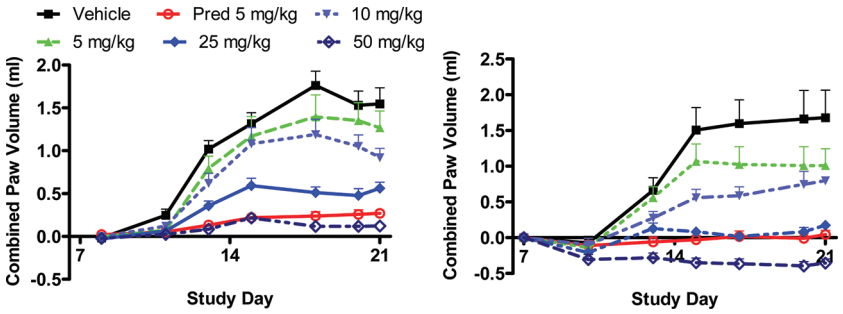

Figure 3. Compounds **35** (left), **37** (right), and pred in the rat adjuvant-induced model of arthritis.

CONCLUSIONS

Studies to address concerns around metabolic liabilities associated with phenols **5** and **6** have led to the identification of a novel series of 5*H*-chromeno[2,3-*b*]pyridine (azaxanthene) GR modulators, which can be efficiently prepared as single enantiomers on multigram scale. Agonist activity was found to be particularly sensitive to the nature of the substituent at the para position of a phenyl ring appended to the C-2 position of the tricyclic azaxanthene core. While potent binding affinity was maintained for this series of ligands, a broad range of pharmacological profiles for both TR and TA was revealed. Tertiary benzamides (e.g., **33**, **35**−**45**) were discovered to be partial agonists of TR and TA, and introduction of a meta halogen consistently attenuated agonist efficacy (e.g., **27**, **28**, **35**, **37**, **38**, **40**, **42**). These partial agonist ligands were also found to competitively antagonize TA induced by **1** in the GAL4 assay, with the extent of maximal antagonism agreeing well with agonist efficacy in the absence of **1**. Modeling studies show that the azaxanthene ligands most likely bind GR utilizing a significantly expanded ligand binding pocket, reminiscent of the reported X-ray structures of **3** and arylpyrazole bound GR.[9] In addition, these ligands appear to take advantage of the "meta channel" identified in the former and probably represent the first ligands since its identification to utilize this surface to effectively modulate receptor function.

Most screening paradigms for the identification of selective GR modulators have relied heavily on cellular assays of TR and TA, in which it has been postulated that ligands that best dissociate these canonical pathways ("dissociated agonists") should provide a favorable clinical risk to benefit ratio.[3] Recent studies have revealed that GR function and GC mechanism of action are significantly more complex than reflected by these dual (TR and TA) pathways. The existence of multiple GR splice variants and polymorphisms, the effects of post-translational receptor modifications, differential recruitment of coactivators/corepressors and other transcriptional regulators, and nongenomic effects have all been suggested to play a role in GC pharmacology.[16] Of particular concern are reports that describe roles for some glucocorticoid-induced gene products (i.e., products of GR-mediated transactivation) in contributing to the anti-inflammatory efficacy of GCs. These findings have led to the suggestion that minimizing GR transactivation, thereby decreasing expression of these gene products, would be expected to negatively impact efficacy.[4] As inhibition of proinflammatory cytokine production is believed to be a fundamental mechanism underlying the clinical efficacy of GCs, we have screened partial agonists through several assays of cytokine production in human whole blood, a highly physiologically relevant assay system. This screening paradigm has allowed for the identification of GR agonist profiles that should have the highest probability of maintaining clinical efficacy. Compounds that were very weak agonists of TA (nearly full antagonists of TA in the GAL4 assay) and that maintained some, albeit weak, activity in TR assays (**27**, **32**, **40**) were found to be very weak inhibitors of cytokine production in all three assays. Partial agonists (**35**−**37**, **42**−**45**) that represented a broad efficacy range in the GAL4 assay (32−76% of dex) generally provided very high efficacy (at or above 80% of dex) in the LPS-induced TNF and IL-1β-induced IL-8 assays, with somewhat lower efficacy for inhibiting TNF-induced IL-8. The significant differences in pharmacology observed with subtle structural differences between ligands in the azaxanthene series is reminiscent of results reported for a series of closely related arylpyrazole-containing GR agonists.[17] Notably, a broad correlation between the capacity of those ligands at a single concentration to activate expression of several genes in A549 cells with their ability to inhibit the expression of inflammatory cytokines in the same cell line was reported. The tertiary benzamide-containing azaxanthenes represent an improvement over the phenols **5** and **6** and even over azaxanthenes not bearing benzamide substituents (e.g., **21** and **23**) in selectivity against the closely related PR. Selectivity over other related nuclear receptors (MR, ERα, and AR) was also maintained for this class of ligands. Compounds **35** and **37** provided sufficient exposures after oral dosing to demonstrate efficacy equivalent to that of a commonly administered steroid (**2**) in both acute and chronic models of arthritis. Studies to address the underlying cause and to improve upon the greater than dose-proportional increases in exposure after oral dosing of both **35** and **37** will be reported in due course. Ultimately, biological studies to evaluate the molecular mechanisms behind the pharmacological profiles of agents like **35** and **37**, coupled with their carefully controlled clinical evaluation, will be most useful in advancing this field.

EXPERIMENTAL SECTION

Chemistry. All commercially available chemicals and solvents were used without further purification. Reactions are performed under an atmosphere of nitrogen. All new compounds gave satisfactory ^{1}H NMR, LC/MS and/or HRMS, and mass spectrometry results. ^{1}H NMR spectra were obtained on a Bruker 400 MHz or a Jeol 500 MHz NMR spectrometer using residual signal of deuterated NMR solvent as internal reference. Electrospray ionization (ESI) mass spectra were obtained on a Water Micromass ESI-MS single quadrupole mass spectrometer. High-resolution mass spectral analysis was performed on an LTQ-FT mass spectrometer interfaced to a Waters Acquity ultraperformance liquid chromatograph. The purity of tested compounds determined by

analytical HPLC was >95% except as noted. Analytical HPLC was performed on a Shimadzu instrument: column, YMC Combiscreen ODS-A, 4.6 mm × 50 mm; gradient elution 0−100% B/A over 4 min with 1 min hold (solvent A, 90% water/10% MeOH/0.2% H_3PO_4; solvent B, 90% MeOH/10% water/0.2% H_3PO_4; flow rate, 4 mL/min; 220 or 254 nm detection wavelength.

5*H*-[1]Benzopyrano[2,3-*b*]pyridin-5-ol (8). To a suspension of 1-azaxanthone (18.5 g, 94 mmol) in MeOH (650 mL) at 0 °C was added sodium borohydride (4.26 g, 113 mmol) portionwise over 10 min. The reaction mixture was allowed to warm to room temperature and stirred for 15 h. HPLC analysis of the reaction mixture indicated two peaks, one corresponding to the alcohol, the other corresponding to 9-methoxy-1-azaxanthene which is presumably generated under the condition of HPLC analysis. The pale yellow solution was then concentrated to one-third volume and poured into cold brine (500 mL). The mixture was washed with chloroform (2 × 300 mL). The combined organic layers were dried over Na_2SO_4 and concentrated to give a yellowish solid **8** (17.80 g, 95% yield) which was used directly in the next step without further purification. ESI-MS m/z 200.21 ($[M + H)^+]$). HPLC t_R = 2.01 min.

α,α-Dimethyl-5*H*-[1]Benzopyrano[2,3-*b*]pyridin-5-acetic Acid Methyl Ester (9). To a suspension of the alcohol **8** (17.80 g, 89 mmol) in dichloromethane (475 mL) at 0 °C was added titanium tetrachloride (1.0 M in dichloromethane, 89 mL, 89 mmol) dropwise. The resulting tan suspension was stirred for 10 min at 0 °C (mechanical stirrer) before adding (1-methoxy-2-methylprop-1-enyloxy)trimethylsilane (36 mL, 173 mmol) to the mixture dropwise. The resulting dark, homogeneous solution was allowed to stir 1 h at 0 °C, then quenched with the addition of saturated aqueous $NaHCO_3$ solution, giving gas evolution and a white precipitate. The mixture was filtered over Celite, and the resulting organic layer of the filtrate was separated, dried over Na_2SO_4, and concentrated to give **9** (22.3 g, 89% yield) as a solid which was used directly in the next step with no further purification. ESI-MS m/z 284 ($[M + H)^+]$). HPLC t_R = 3.04 min.

method A. Synthesis of α,α-Dimethyl-*N*-1,3,4-thiadiazol-2-yl-5*H*-[1]benzopyrano[2,3-*b*]pyridine-5-acetamide (10). *a.* To a solution of **9** (1.0 g, 3.53 mmol) in THF (10 mL) and methanol (10 mL) was added a solution of KOH (0.99 g, 17.65 mmol) in water (10 mL). The resulting solution was heated at reflux (65 °C) for 10 h, then concentrated under reduced pressure to about $^2/_3$ volume. The resulting solution was acidified to pH 5 with the dropwise addition of 1 N HCl, then washed with ethyl acetate (2 × 10 mL). The combined organic layers were dried over Na_2SO_4 and concentrated to provide the α,α-dimethyl-5*H*-[1]benzopyrano[2,3-*b*]pyridin-5-acetic acid as a white solid (0.90 g, 95% yield). ESI-MS m/z 270.02 ($[M + H]^+$). HPLC t_R = 2.84 min.

b. To a solution of the carboxylic acid (150 mg, 0.56 mmol) in anhydrous acetonitrile (3.0 mL) was added EDC (128 mg, 0.67 mmol), HOAt (91 mg, 0.67 mmol), 2-amino-1,3,4-thiadiazole (68 mg, 0.67 mmol), and diisopropylethylamine (0.36 mL, 2.01 mmol). The resulting mixture was stirred at 80 °C for 1 h and at room temperature overnight, then concentrated in vacuo. The residue was mixed with ethyl acetate (6 mL), washed with water (5 mL) and saturated aqueous $NaHCO_3$ solution (2 × 5 mL), dried over Na_2SO_4, and concentrated in vacuo. Purification using preparative HPLC gave the product **10** (150 mg, 77% yield) as a white solid. ^{1}H NMR (400 MHz, CD_3OD) δ 8.39 (s, 1H), 8.23 (dd, J = 4.8, 1.8 Hz, 1H), 7.72 (dd, J = 7.6, 1.5 Hz, 1H), 7.42−7.34 (m, 1H), 7.31−7.18 (m, 3H), 7.13 (dd, J = 7.4, 1.3 Hz, 1H), 4.62 (s, 1H), 1.16 (d, J = 9.2 Hz, 6H). ESI-MS m/z 353.19 ($[M + H]^+$). HPLC t_R = 2.81 min.

2-Chloro-α,α-dimethyl-5*H*-[1]benzopyrano[2,3-*b*]pyridin-5-acetic Acid Methyl Ester (11). *a.* To a solution of the ester **9** (21.2 g, 74.9 mmol) in dichloromethane at room temperature was added mCPBA (containing 30% m-chlorobenzoic acid) (53 g). After 2 h, the reaction mixture was washed sequentially with 10% aqueous sodium sulfite (500 mL), 1 N aqueous NaOH (200 mL), and water (200 mL). The organic layer was dried over Na_2SO_4 and concentrated to provide the α,α-dimethyl-5*H*-[1]benzopyrano[2,3-*b*]pyridin-5-acetic acid methyl ester 1-oxide as an amorphous solid (21.63 g, 97% yield) which was used directly in the next step with no further purification. ESI-MS m/z 300 ($[M + H]^+$). HPLC t_R = 2.25 min.

b. A solution of the *N*-oxide intermediate (21.15 g, 71.0 mmol) in phosphorus oxychloride (150 mL) was heated for 30 min at 90 °C. The solvent was then removed by vacuum bulb-to-bulb distillation. The residual solid was dissolved in dichloromethane (250 mL) and transferred portionwise to a 1 L beaker containing ice. Solid Na_2CO_3 was added in portions with vigorous stirring (gas evolved) to the resulting slurry until it reached pH 6. The resulting emulsion was allowed to sit overnight in a separatory funnel. The organic layer was removed, dried over Na_2SO_4, and concentrated to give the crude solid which was recrystallized from methanol to give the chloride **11** (17.37 g, 77% yield) as a solid. ESI-MS m/z 318 ($[M + H]^+$). HPLC t_R = 3.37 min.

method B. (*S*)-2-Chloro-5*H*-chromeno[2,3-*b*]pyridine-5-yl)-2-methylpropanoic Acid (12a) and (*R*)-2-Chloro-5*H*-chromeno[2,3-*b*]pyridine-5-yl)-2-methylpropanoic Acid (12b). *a.* To a solution of the chloropyridine (16.08 g, 50.7 mmol) in THF (240 mL) and methanol (400 mL) was added a solution of KOH (28.46 g, 507 mmol) in water (320 mL). The resulting solution was heated at reflux (65 °C) 10 h, then concentrated under reduced pressure to about $^2/_3$ volume. The resulting solution was acidified to pH 5 with the dropwise addition of 12 N HCl, then washed with ethyl acetate (2 × 300 mL). The combined organic layers were dried (Na_2SO_4) and concentrated. The crude carboxylic acid (12.6 g) was dissolved in warm ethyl acetate (600 mL) and treated with benzylamine (9.2 mL, 48 mmol). The solution was allowed to gradually cool to room temperature and allowed to sit for 3 h. The precipitate was collected and washed (diethyl ether), then partitioned between ethyl acetate (350 mL) and 1 N aqueous HCl (200 mL). The organic layer was dried over magnesium sulfate and concentrated to provide a racemic acid as a solid (8.53 g, 43% yield for two steps). ESI-MS m/z 304 ($[M + H]^+$). HPLC t_R = 3.19 min.

b. The racemic acid was resolved into its corresponding enantiomers using chiral supercritical fluid chromatography (SFC) with the following conditions: column, ChiralCEL OJ 250 mm × 4.6 mm 10 μm; mobile phase, CO_2/MeOH = 85/15, 100 bar; temperature, 35 °C; flow rate, 2 mL/min; detection, UV (254 and 220 nm). Retention time: first enantiomer, 4.74 min (>98% ee); second eluting enantiomer, 6.75 min (>99% ee).

A sample of the first eluting enantiomer **12b** was cocrystallized with (*R*)-(+)-α-methylbenzylamine in ethyl acetate (CH_3COOEt). An X-ray structure determination of the crystalline material thus obtained proved **12b** to be of (*R*) absolute stereochemistry. The absolute configuration of the second-eluting enantiomer **12a** is deduced to be (*S*).

method C. Synthesis of [(5*S*)-2-Phenyl-α,α-dimethyl-*N*-1,3,4-thiadiazol-2-yl-5*H*-[1]benzopyrano[2,3-*b*]pyridin-5-acetamide 14. *a.* To a solution of (*S*)-2-(2-chloro-5*H*-chromeno[2,3-*b*]-pyridin-5-yl)-2-methylpropanoic acid (**12a**, 10 g, 32.9 mmol) in acetonitrile (200 mL) were added triethylamine (22.94 mL, 165 mmol), HATU (16.27 g, 42.8 mmol), and 1,3,4-thiadiazol-2-amine (9.99 g, 99 mmol). The resulting mixture was heated at 80 °C for 3 h and at room temperature overnight. The mixture was concentrated in vacuo, and the residue was partitioned between EtOAc and 1 N HCl. The obtained organic layer was washed with saturated $NaHCO_3$, brine, then dried (Na_2SO_4) and concentrated to give a solid. The solid was dissolved in EtOH (400 mL) with gentle warming. Then 1 N HCl (~200 mL) was added portionwise. The solid was collected and washed with water, dried on vacuum pump overnight to give product (5*S*)-2-chloro-α,α-dimethyl-*N*-1,3,4-thiadiazol-2-yl-5*H*-[1]benzopyrano[2,3-*b*]pyridin-5-acetamide **13** (10 g, 79% yield). ESI-MS m/z 387 ($[M + H]^+$). HPLC t_R = 3.12 min.

b. A DMF (50 mL) solution of **13** (30 mg, 0.078 mmol), phenylboronic acid (24 mg, 0.156 mmol), $Pd(Ph_3P)_4$ (10 mg, 0.12 equiv), and a 2 M solution of K_3PO_4 (0.2 mL, 5 equiv) was degassed by vacuum−N_2 refill cycle twice and then heated at 100 °C under N_2 for 5 h. After the mixture was cooled to room temperature, the crude material was poured into 1 N HCl and extracted with ethyl acetate. The ethyl acetate phase was washed with water and brine, dried over $MgSO_4$, and filtered. The filtrate was purified by prep-arative HPLC to give **14** (25 mg, 70% yield). ^{1}H NMR (400 MHz, $CDCl_3$) δ 8.91 (s, 1H), 8.10−8.01 (m, 2H), 7.70 (d, J = 7.6 Hz, 1H), 7.57−7.41 (m, 4H), 7.39−7.31 (m, 2H), 7.20 (d, J = 7.1 Hz, 1H), 7.11−7.01 (m, 1H), 4.70 (s, 1H), 1.28 (d, J = 11.2 Hz, 6H). ESI-MS m/z 429.17 ($[M + H]^+$). HPLC t_R = 3.06 min.

[(5*S*)-2-[(2-Methyl)phenyl]-α,α-dimethyl-*N*-1,3,4-thiadiazol-2-yl-5*H*-[1]benzopyrano[2,3-*b*]pyridin-5-acetamide 15. **15** was prepared from **13** according to method C, step b. ^{1}H NMR (400 MHz, $CDCl_3$) δ 8.89 (s, 1H), 7.70 (d, J = 7.7 Hz, 1H), 7.46−7.41 (m, 1H), 7.27 (s, 5H), 7.22−7.16 (m, 2H), 7.09−7.03 (m, 1H), 4.70 (s, 1H), 2.38 (s, 3H), 1.29 (d, J = 12.5 Hz, 6H). ESI-MS m/z 443.10 ($[M + H]^+$). HPLC t_R = 3.44 min.

[(5*S*)-2-[(3-Methyl)phenyl]-α,α-dimethyl-*N*-1,3,4-thiadiazol-2-yl-5*H*-[1]benzopyrano[2,3-*b*]pyridin-5-acetamide 16. **16** was prepared from **13** according to method C, step b. ^{1}H NMR (400 MHz, $CDCl_3$) δ 8.87 (s, 1H), 7.87 (s, 1H), 7.77 (d, J = 7.7 Hz, 1H), 7.64 (d, J = 7.9 Hz, 1H), 7.52 (d, J = 7.9 Hz, 1H), 7.40−7.31 (m, 3H), 7.24 (s, 1H), 7.16−7.09 (m, 1H), 7.09−7.02 (m, 1H), 4.53 (s, 1H), 2.44 (s, 3H), 1.26 (d, J = 15.2 Hz, 6H). ESI-MS m/z 443.09 ($[M + H]^+$). HPLC t_R = 3.59 min.

[(5*S*)-2-[(4-Methyl)phenyl]-α,α-dimethyl-*N*-1,3,4-thiadiazol-2-yl-5*H*-[1]benzopyrano[2,3-*b*]pyridin-5-acetamide 17. **17** was prepared from **13** according to method C, step b. ^{1}H NMR (400 MHz, $CDCl_3$) δ 8.83 (s, 1H), 7.86 (d, J = 8.1 Hz, 2H), 7.63 (d, J = 8.1 Hz, 1H), 7.41 (d, J = 7.6 Hz, 1H), 7.28−7.20 (m, 3H), 7.18 (br s, 1H), 7.14 (d, J = 7.6 Hz, 1H), 7.02−6.90 (m, 1H), 4.67 (s, 1H), 2.33 (s, 3H), 1.19 (d, J = 13.2 Hz, 6H). ESI-MS m/z 443.40 ($[M + H]^+$). HPLC t_R = 3.81 min.

[(5*R*)-2-(4-Methoxyphenyl)-α,α-dimethyl-*N*-1,3,4-thiadiazol-2-yl-5*H*-[1] benzopyrano [2,3-*b*]pyridin-5-acetamide 18. **18** was prepared from **12b** according to method C. ^{1}H NMR (400 MHz, $CDCl_3$) δ 8.90 (s, 1H), 8.06−7.97 (m, 2H), 7.64 (d, J = 7.6 Hz, 1H), 7.46 (d, J = 7.6 Hz, 1H), 7.38−7.29 (m, 2H), 7.18 (d, J = 7.1 Hz, 1H), 7.09−6.97 (m, 3H), 4.64 (s, 1H), 3.89 (s, 3H), 1.27 (d, J = 12.2 Hz, 6H). ESI-MS m/z 459.32 ($[M + H]^+$). HPLC t_R = 3.65 min.

(5*S*)-2-(4-Methoxyphenyl)-α,α-dimethyl-*N*-1,3,4-thiadiazol-2-yl-5*H*-[1]benzopyrano[2,3-*b*]pyridin-5-acetamide 19. **19** was prepared from **13** according to method C, step b. ^{1}H NMR (400 MHz, $CDCl_3$) δ 8.83 (s, 1H), 7.98−7.87 (m, 2H), 7.61 (d, J = 8.1 Hz, 1H), 7.37 (d, J = 7.6 Hz, 1H), 7.29−7.18 (m, 2H), 7.14 (d, J = 7.6 Hz, 1H), 7.02−6.85 (m, 3H), 4.67 (s, 1H), 3.79 (s, 3H), 1.20 (d, J = 13.2 Hz, 6H). ESI-MS m/z 459.19 $(M + H)^+$. HPLC t_R = 3.63 min.

[(5*S*)-2-[(4-Ethyl)phenyl]-α,α-dimethyl-*N*-1,3,4-thiadiazol-2-yl-5*H*-[1]benzopyrano[2,3-*b*]pyridin-5-acetamide 20. **20** was prepared from **13** according to method C, step b. ^{1}H NMR (400 MHz, $CDCl_3$) δ 8.87 (s, 1H), 7.95−7.89 (m, 2H), 7.64 (d, J = 7.9 Hz, 1H), 7.50 (d, J = 7.7 Hz, 1H), 7.34−7.28 (m, 4H), 7.15−7.09 (m, 1H), 7.08−7.01 (m, 1H), 4.54 (s, 1H), 2.72 (q, J = 7.7 Hz, 2H), 1.33−1.22 (m, 9H). ESI-MS m/z 457.06 ($[M + H]^+$). HPLC t_R = 3.74 min.

[(5*S*)-2-[(4-Propyl)phenyl]-α,α-dimethyl-*N*-1,3,4-thiadiazol-2-yl-5*H*-[1]benzopyrano[2,3-*b*]pyridin-5-acetamide 21. **21** was prepared from **13** according to method C, step b. ^{1}H NMR (400 MHz, $CDCl_3$) δ 8.88 (s, 1H), 7.94 (d, J = 8.4 Hz, 2H), 7.67−7.63 (m, 1H), 7.49 (d, J = 7.7 Hz, 2H), 7.32−7.28 (m, 3H), 7.15 (d, J = 7.5 Hz, 1H), 7.08−7.01 (m, 1H), 4.62 (s, 1H), 2.65 (t, J = 7.6 Hz, 2H), 1.75−1.61 (m, 2H), 1.26 (d, J = 14.1 Hz, 6H), 1.01−0.92 (m, 3H). ESI-MS m/z 471.13 ($[M + H]^+$). HPLC t_R = 3.91 min.

[(5*S*)-α,α-Dimethyl-2-[(4-methylethooxy)phenyl]-*N*-1,3,4-thiadiazol-2-yl-5*H*-[1]benzopyrano[2,3-*b*]pyridin-5-acetamide 22. **22** was prepared from **13** according to method C, step b. ^{1}H NMR (400 MHz, $CDCl_3$) δ 8.88 (s, 1H), 8.00−7.93 (m, 2H), 7.63 (d, J = 7.7 Hz, 1H), 7.44 (d, J = 7.9 Hz, 1H), 7.35−7.28 (m, 2H), 7.16 (d, J = 7.3 Hz, 1H), 7.08−7.01 (m, 1H), 7.00−6.93 (m, 2H), 4.69−4.58 (m, 2H), 1.37 (d, J = 5.9 Hz, 6H), 1.26 (d, J = 13.0 Hz, 6H). ESI-MS m/z 487.13 ($[M + H]^+$). HPLC t_R = 3.69 min.

[(5*S*)-α,α-Dimethyl-2-[(4-hydroxyl)phenyl]-*N*-1,3,4-thiadiazol-2-yl-5*H*-[1]benzopyrano[2,3-*b*]pyridin-5-acetamide 23. **23** was prepared from **13** according to method C, step b. ^{1}H NMR (400 MHz, $CDCl_3$) δ 8.88 (s, 1H), 7.97−7.90 (m, 2H), 7.60 (d, J = 8.1 Hz, 1H), 7.42 (d, J = 7.7 Hz, 1H), 7.35−7.29 (m, 2H), 7.16 (d, J = 7.3 Hz, 1H), 7.09−7.01 (m, 1H), 6.95−6.89 (m, 2H), 4.58 (s, 1H), 1.25 (d, J = 5.3 Hz, 6H). ESI-MS m/z 445.08 ($[M + H]^+$). HPLC t_R = 3.06 min.

[(5*S*)-2-[4-(*N*,*N*-Dimethylphenyl]-α,α-dimethyl-*N*-1,3,4-thiadiazol-2-yl-5*H*-[1]benzopyrano[2,3-*b*]pyridin-5-acetamide 24. **24** was prepared from **13** according to method C, step b. ^{1}H NMR (400 MHz, $CDCl_3$) δ 8.87 (s, 1H), 8.14 (d, J = 8.8 Hz, 2H), 7.67 (d, J = 7.7 Hz, 1H), 7.56−7.48 (m, 3H), 7.37−7.31 (m, 2H), 7.18−7.05 (m, 2H), 3.99 (s, 1H), 3.24 (s, 6H), 1.23 (d, J = 6.0 Hz, 6H). ESI-MS m/z 472.12($[M + H]^+$). HPLC t_R = 3.09 min.

[(5*S*)-2-[4-(Ethylsulfonyl))phenyl]-α,α-dimethyl-*N*-1,3,4-thiadiazol-2-yl-5*H*-[1]benzopyrano[2,3-*b*]pyridin-5-acetamide 25. **25** was prepared from **13** according to method C, step b. ^{1}H NMR (400 MHz, $CDCl_3$) δ 8.90 (s, 1H), 8.23 (d, J = 8.3 Hz, 2H), 8.00 (d, J = 8.6 Hz, 2H), 7.74 (d, J = 7.8 Hz, 1H), 7.58 (d, J = 7.8 Hz, 1H), 7.34 (d, J = 4.0 Hz, 2H), 7.21 (d, J = 7.6 Hz, 1H), 7.09 (dd, J = 7.8, 4.3 Hz, 1H), 4.71 (s, 1H), 3.17 (q, J = 7.6 Hz, 2H), 1.37−1.22 (m, 9H). ESI-MS m/z 521.31 ($[M + H]^+$). HPLC t_R = 3.26 min.

[(5*S*)-2-(4-Acetylphenyl)-α,α-dimethyl-*N*-1,3,4-thiadiazol-2-yl-5*H*-[1]benzopyrano[2,3-*b*]pyridin-5-acetamide 26. **26** was prepared from **13** according to method C, step b. ^{1}H NMR (400 MHz, $CDCl_3$) δ 8.90 (s, 1H), 8.18−8.12 (m, 2H), 8.09−8.02 (m, 2H), 7.74 (d, J = 7.9 Hz, 1H), 7.57 (d, J = 7.9 Hz, 1H), 7.38−7.31 (m, 2H), 7.23 (d, J = 7.0 Hz, 1H), 7.10−7.04 (m, 1H), 4.75 (s, 1H), 2.66 (s, 3H), 1.28 (d, J = 4.4 Hz, 6H). ESI-MS m/z 471.10 ($[M + H]^+$). HPLC t_R = 3.27 min.

[(5*S*)-2-[3-Fluoro-4-(1-methylethoxy)phenyl]-α,α-dimethyl-*N*-1,3,4-thiadiazol-2-yl-5*H*-[1]benzopyrano[2,3-*b*]pyridin-5-acetamide 27. **27** was prepared from **13** according to method C, step b. ^{1}H NMR (400 MHz, $CDCl_3$) δ 8.89 (s, 1H), 7.84−7.73 (m, 2H), 7.64 (d, J = 7.6 Hz, 1H), 7.41 (d, J = 7.6 Hz, 1H), 7.34−7.30 (m, 2H), 7.19 (d, J = 7.1 Hz, 1H), 7.08−7.01 (m, 2H), 4.69−4.60 (m, 2H), 1.40 (d, J = 6.1 Hz, 6H), 1.30−1.18 (m, 6H). ESI-MS m/z 505.05 ($[M + H]^+$). HPLC t_R = 3.92 min.

[(5*S*)-2-(4-Acetyl-3-fluorophenyl)-α,α-dimethyl-*N*-1,3,4-thiadiazol-2-yl-5*H*-[1]benzopyrano[2,3-*b*]pyridin-5-acetamide 28. **28** was prepared from **13** according to method C, step b. ^{1}H NMR (400 MHz, $CDCl_3$) δ 8.89 (s, 1H), 8.01−7.95 (m, 1H), 7.93−7.84 (m, 2H), 7.71 (d, J = 7.8 Hz, 1H), 7.55 (d, J = 7.6 Hz, 1H), 7.37−7.33 (m, 2H), 7.19 (d, J = 7.6 Hz, 1H), 7.11−7.05 (m, 1H), 4.69 (s, 1H), 2.70 (d, J = 4.8 Hz, 3H), 1.26 (s, 6H). ESI-MS m/z 489.09 ($[M + H]^+$). HPLC t_R = 3.65 min.

4-[(5*S*)-5-[1,1-Dimethyl-2-oxo-2-(1,3,4-thiadiazol-2-ylamino)-ethyl]-5*H*-[1]benzopyrano[2,3-*b*]pyridin-2-yl]benzoic Acid 29a. **29a** was prepared from **13** according to method C, step b. ^{1}H NMR (400 MHz, CD_3OD) δ 9.12 (s, 1H), 8.20−8.12 (m, 4H), 8.00 (s, 1H), 7.81−7.71 (m, 2H), 7.43−7.36 (m, 1H), 7.33−7.24 (m, 2H), 7.19−7.10 (m, 1H), 4.66 (s, 1H), 1.20 (d, J = 9.7 Hz, 6H). ESI-MS m/z 473.13 ($[M + H]^+$). HPLC t_R = 3.42 min.

4-[(5*S*)-5-[1,1-Dimethyl-2-oxo-2-(1,3,4-thiadiazol-2-ylamino)-ethyl]-5*H*-[1]benzopyrano[2,3-*b*]pyridin-2-yl]-2-fluorobenzoic Acid 29b. **29b** was prepared from **13** according to method C, step

b. ^{1}H NMR (400 MHz, CD_3OD) δ 8.95 (s, 1H), 8.09−8.01 (m, 1H), 7.88−7.80 (m, 2H), 7.69 (d, J = 7.9 Hz, 1H), 7.57 (d, J = 7.7 Hz, 1H), 7.37−7.27 (m, 2H), 7.18 (d, J = 7.0 Hz, 1H), 7.09 (dd, J = 6.7, 1.9 Hz, 1H), 4.62 (s, 1H), 1.20 (d, J = 9.9 Hz, 6H). ESI-MS m/z 491 ($[M + H]^+$). HPLC t_R = 3.31 min.

4-[(5*S*)-5-[1,1-Dimethyl-2-oxo-2-(1,3,4-thiadiazol-2-ylamino)-ethyl]-5*H*-[1]benzopyrano[2,3-*b*]pyridin-2-yl]-2-chlorobenzoic Acid 29c. **29c** was prepared from **13** according to method C, step b. ^{1}H NMR (400 MHz, CD_3OD) δ 8.96 (s, 1H), 8.13 (d, J = 0.9 Hz, 1H), 8.00−7.91 (m, 2H), 7.69 (d, J = 7.9 Hz, 1H), 7.56 (d, J = 7.7 Hz, 1H), 7.38−7.27 (m, 2H), 7.18 (s, 1H), 7.13−7.04 (m, 1H), 4.62 (s, 1H), 1.20 (d, J = 9.2 Hz, 6H). ESI-MS m/z 506.98 ($[M + H]^+$). HPLC t_R = 3.31 min.

Method D. Synthesis of [(5*S*)-2-[4-(Aminocarbonyl)-phenyl]-α,α-dimethyl-*N*-1,3,4-thiadiazol-2-yl-5*H*-[1]benzopyrano-[2,3-*b*]pyridin-5-acetamide 30. A solution of the benzoic acid **29a** (31 mg, 0.066 mmol), triethylamine (0.028 mL, 0.20 mmol), HOBT monohydrate (12 mg, 0.086 mmol), EDC (16 mg, 0.086 mmol), and ammonium chloride (11 mg, 0.208 mmol) in acetonitrile (1.0 mL) was heated for 12 h at 45 °C. Purification by preparative HPLC gave the desired product **30** (15 mg, 35%), which was lyophilized from acetonitrile/water to give an amorphous, white solid. ^{1}H NMR (500 MHz, CD_3OD) δ 8.89 (s, 1H), 8.07 (d, J = 8.2 Hz, 2H), 7.87 (d, J = 8.2 Hz, 2H), 7.68 (d, J = 7.7 Hz, 1H), 7.53 (d, J = 7.7 Hz, 1H), 7.31 (d, J = 3.3 Hz, 2H), 7.20 (d, J = 7.7 Hz, 1H), 7.11−7.04 (m, 1H), 4.69 (s, 1H), 1.26 (d, J = 3.8 Hz, 6H). ESI-MS m/z 472.19 ($[M + H]^+$). HPLC t_R = 3.03 min.

[(5*S*)-2-[4-[(Methylamino)carbonyl)]phenyl]-α,α-dimethyl-*N*-1,3,4-thiadiazol-2-yl-5*H*-[1]benzopyrano[2,3-*b*]pyridin-5-acetamide 31. **31** was prepared from **29a** according to method D. ^{1}H NMR (500 MHz, CD_3OD) δ 8.86 (s, 1H), 8.09 (d, J = 8.2 Hz, 2H), 7.85 (d, J = 8.2 Hz, 2H), 7.65 (d, J = 7.7 Hz, 1H), 7.56 (d, J = 7.7 Hz, 1H), 7.35−7.29 (m, 2H), 7.14−7.09 (m, 1H), 7.09−7.04 (m, 1H), 4.52 (s, 1H), 3.07 (d, J = 4.9 Hz, 3H), 1.25 (d, J = 15.4 Hz, 6H). ESI-MS m/z 486.16 ($[M + H]^+$). HPLC t_R = 3.17 min.

[(5*S*)-2-[4-[(Methylamino)carbonyl)]-3-fluorophenyl]-α,α-dimethyl-*N*-1,3,4-thiadiazol-2-yl-5*H*-[1]benzopyrano[2,3-*b*]-pyridin-5-acetamide 32. **32** was prepared from **29a** according to method D. ^{1}H NMR (400 MHz, $CDCl_3$) δ 8.91 (s, 1H), 8.20 (t, J = 8.2 Hz, 1H), 7.96−7.85 (m, 2H), 7.75 (d, J = 7.6 Hz, 1H), 7.57 (d, J = 7.8 Hz, 1H), 7.37−7.30 (m, 2H), 7.21 (d, J = 7.6 Hz, 1H), 7.15−7.04 (m, 1H), 6.92 (dd, J = 13.1, 4.8 Hz, 1H), 4.71 (s, 1H), 3.08 (d, J = 4.5 Hz, 3H), 1.29 (d, J = 9.8 Hz, 6H). ESI-MS m/z 504.15 ($[M + H]^+$). HPLC t_R = 3.16 min.

[(5*S*)-2-[4-[(Dimethylamino)carbonyl]phenyl]-α,α-dimethyl-*N*-1,3,4-thiadiazol-2-yl-5*H*-[1]benzopyrano[2,3-*b*]pyridin-5-acetamide 33. **33** was prepared from **13** according to method C, step b. ^{1}H NMR (400 MHz, $CDCl_3$) δ ppm 8.85 (1 H, s), 7.99 (2 H, d, J = 8.6 Hz), 7.69 (1 H, d, J = 7.6 Hz), 7.38−7.52 (3 H, m), 7.11−7.32 (3 H, m), 6.88−7.07 (1 H, m), 4.79 (1 H, s), 3.07 (3 H, br s), 2.93 (3 H, br s), 1.21 (6 H, d, J = 9.2 Hz). ESI-MS m/z 500.21 ($[M + H]^+$). HPLC t_R = 3.22 min.

[(5*R*)-2-[4-[(Dimethylamino)carbonyl]phenyl]-α,α-dimethyl-*N*-1,3,4-thiadiazol-2-yl-5*H*-[1]benzopyrano[2,3-*b*]pyridin-5-acetamide 34. **34** was prepared from **12b** according to method C. ^{1}H NMR (400 MHz, $CDCl_3$) δ 8.90 (s, 1H), 8.09 (d, J = 8.1 Hz, 2H), 7.69 (d, J = 7.6 Hz, 1H), 7.55 (d, J = 8.1 Hz, 3H), 7.38−7.32 (m, J = 3.6 Hz, 2H), 7.18 (d, J = 7.6 Hz, 1H), 7.12−7.03 (m, 1H), 4.63 (s, 1H), 3.17 (br s, 3H), 3.04 (br s, 3H), 1.27 (d, J = 9.2 Hz, 6H). ESI-MS m/z 500.16 ($[M + H]^+$). HPLC t_R = 3.22 min.

[(5*S*)-2-[4-[(Dimethylamino)carbonyl]-3-fluorophenyl]-α,α-dimethyl-*N*-1,3,4-thiadiazol-2-yl-5*H*-[1]benzopyrano[2,3-*b*]-pyridin-5-acetamide 35. **35** was prepared from **29b** according to method D. ^{1}H NMR (500 MHz, DMSO-d_6) δ ppm 12.67 (1 H, br s), 9.24 (1 H, s), 8.03 (1 H, dd, J = 8.11, 1.51 Hz), 7.99 (1 H, dd, J = 11.13, 1.24 Hz), 7.90 (1 H, d, J = 7.70 Hz), 7.67 (1 H, d, J = 7.97 Hz), 7.51 (1 H, t, J = 7.56 Hz), 7.37 (1 H, ddd, J = 8.25, 6.60, 2.20 Hz), 7.31 (1 H, d, J = 7.97 Hz), 7.15−7.19 (1 H, m), 7.11−7.16 (1 H, m), 4.85 (1 H, s), 3.03 (3 H, s), 2.89 (3 H, s), 1.06 (3 H, s), 1.04 (3 H, s). ^{13}C NMR (126 MHz, DMSO-d_6) δ ppm 174.17, 164.94, 158.92 (2 C, s), 157.99 (1 C, d, J = 259.40 Hz), 152.53, 151.48, 148.97, 140.34−140.44 (1 C, m), 140.27, 129.20 (2 C, br s), 128.79, 125.18 (1 C, d, J = 17.80 Hz), 123.88, 122.66, 120.92, 116.74, 116.58, 116.03, 113.37 (1 C, d, J = 22.89 Hz), 49.66, 44.61, 37.69, 34.19, 20.93, 20.69. ^{19}F NMR (471 MHz, DMSO-d_6) δ ppm −115.75 (1 F, t, J = 7.27 Hz). ESI-MS m/z 508.16 ($[M + H]^+$). HPLC t_R = 3.24 min. HRMS m/z calcd for $C_{27}H_{24}FO_3N_5S$ $[(M + H)^+]$ 518.1657, found 518.1664.

[(5*S*)-2-[4-[(Ethylmethylamino)carbonyl]-3-phenyl]-α,α-dimethyl-*N*-1,3,4-thiadiazol-2-yl-5*H*-[1]benzopyrano[2,3-*b*]-pyridin-5-acetamide 36. **36** was prepared from **29a** according to method D. ^{1}H NMR (400 MHz, $CDCl_3$) δ 8.90 (s, 1H), 8.06 (d, J = 8.4 Hz, 2H), 7.71 (d, J = 7.9 Hz, 1H), 7.56−7.45 (m, 3H), 7.35−7.29 (m, 2H), 7.20 (d, J = 7.7 Hz, 1H), 7.10−7.02 (m, 1H), 4.73 (s, 1H), 3.71−3.23 (m, 2H), 3.19−2.92 (m, 3H), 1.36−1.11 (m, 9H). ESI-MS m/z 514.15 ($[M + H]^+$). HPLC t_R = 3.20 min.

[(5*S*)-2-[4-[(Ethylmethylamino)carbonyl]-3-fluorophenyl]-α,α-dimethyl-*N*-1,3,4-thiadiazol-2-yl-5*H*-[1]benzopyrano-[2,3-*b*]pyridin-5-acetamide 37. **37** was prepared from **29b** according to method D. ^{1}H NMR (500 MHz, DMSO-d_6) δ ppm 12.67 (2 H, br s), 9.24 (2 H, s), 8.03 (2 H, ddd, J = 7.97, 3.16, 1.51 Hz), 7.99 (2 H, dt, J = 11.07, 1.75 Hz), 7.90 (2 H, dd, J = 7.70, 1.92 Hz), 7.67 (2 H, d, J = 7.70 Hz), 7.50 (2 H, t, J = 7.56 Hz), 7.37 (2 H, ddd, J = 8.25, 6.60, 2.20 Hz), 7.31 (2 H, d, J = 7.97 Hz), 7.16−7.18 (2 H, m), 7.11−7.16 (2 H, m), 4.85 (2 H, s), 3.51 (2 H, q, J = 7.06 Hz), 3.19 (2 H, q, J = 7.06 Hz), 3.00 (3 H, s), 2.85 (3 H, s), 1.16 (3 H, t, J = 7.01 Hz), 1.06 (6 H, s), 1.04 (6 H, s), 1.02−1.05 (3 H, m). ^{13}C NMR (126 MHz, DMSO-d_6) δ ppm 174.25 (2 C, br s), 164.80 (1 C, s), 164.56 (1 C, s), 159.10 (2 C, br s), 158.94 (2 C, s), 157.88 (2 C, d, J = 241.60 Hz), 152.57 (2 C, s), 151.52 (2 C, s), 148.93 (2 C, br s), 140.29 (2 C, s), 140.16 (2 C, d, J = 7.63 Hz), 129.25 (2 C, s), 129.07 (2 C, br s), 128.79 (2 C, br s), 125.47 (2 C, d, J = 20.34 Hz), 123.88 (2 C, br s), 122.70 (2 C, br s), 120.96 (2 C, s), 116.72 (2 C, s), 116.60 (2 C, s), 116.03 (2 C, br s), 113.43 (1 C, d, J = 22.89 Hz), 113.39 (1 C, d, J = 22.89 Hz), 49.68 (2 C, s), 44.81 (1 C, br s), 44.65 (2 C, s), 41.17 (1 C, s), 35.12 (1 C, s), 31.32 (1 C, s), 20.97 (2 C, br s), 20.71 (2 C, s), 13.12 (1 C, s), 11.85 (1 C, s). ^{19}F NMR (471 MHz, DMSO-d_6) δ ppm −116.12 (1 F, t, J = 7.27 Hz), −116.21 (1 F, t, J = 7.26 Hz). ESI-MS m/z 532.20 ($[M + H]^+$). HPLC t_R = 3.47 min. HRMS m/z calcd for $C_{28}H_{26}O_3N_5FS$ $[(M + H)^+]$ 532.1813, found 532.1814.

[(5*S*)-2-[4-[(Ethylmethylamino)carbonyl]-3-chlorophenyl]-α,α-dimethyl-*N*-1,3,4-thiadiazol-2-yl-5*H*-[1]benzopyrano-[2,3-*b*]pyridin-5-acetamide 38. **38** was prepared from **29c** according to method D. ^{1}H NMR (400 MHz, $CDCl_3$) δ 8.92 (s, 1H), 8.14−7.92 (m, 2H), 7.70 (d, J = 7.8 Hz, 1H), 7.56−7.44 (m, 2H), 7.36−7.30 (m, 2H), 7.20 (d, J = 7.6 Hz, 1H), 7.14−7.03 (m, 1H), 4.71 (br s, 1H), 3.90−3.48 (m, 1H), 3.26 (dq, J = 13.9, 7.2 Hz, 1H), 3.20−2.88 (m, 3H), 1.36−1.10 (m, 9H). ESI-MS m/z 548.20 ($[M + H]^+$). HPLC t_R = 3.44 min.

[(5*S*)-α,α-Dimethyl-2-[4-(1-piperidinylcarbonyl)phenyl]-*N*-1,3,4-thiadiazol-2-yl-5*H*-[1]benzopyrano[2,3-*b*]pyridin-5-acetamide 39. **39** was prepared from **29a** according to method D. ^{1}H NMR (400 MHz, $CDCl_3$) δ 8.90 (s, 1H), 8.06 (d, J = 8.1 Hz, 2H), 7.71 (d, J = 7.6 Hz, 1H), 7.57−7.46 (m, 3H), 7.38−7.30 (m, 2H), 7.21 (d, J = 7.1 Hz, 1H), 7.12−7.02 (m, 1H), 4.73 (s, 1H), 3.75 (br s, 2H), 3.37 (br s, 2H), 1.79−1.48 (m, 6H), 1.27 (d, J = 10.2 Hz, 6H). ESI-MS m/z 549.20 ($[M + H]^+$). HPLC t_R = 3.54 min.

[(5*S*)-2-[3-Fluoro-4-(1-piperidinylcarbonyl)phenyl]-α,α-dimethyl-*N*-1,3,4-thiadiazol-2-yl-5*H*-[1]benzopyrano[2,3-*b*]-pyridin-5-acetamide 40. **40** was prepared from **29b** according to method D. ^{1}H NMR (400 MHz, $CDCl_3$) δ 8.89 (s, 1H), 7.89−7.80

(m, 2H), 7.69 (d, J = 7.6 Hz, 1H), 7.55−7.45 (m, 2H), 7.35 (d, J = 3.6 Hz, 2H), 7.19−7.14 (m, 1H), 7.12−7.06 (m, 1H), 4.66 (s, 1H), 3.78 (br s, 2H), 3.31 (br s, 2H), 1.75−1.52 (m, 6H), 1.28 (d, J = 9.2 Hz, 6H). ESI-MS m/z 558.05 ($[M + H]^+$). HPLC t_R = 3.62 min.

[(5*S*)-α,α-Dimethyl-2-[4-(1-morpholinylcarbonyl)phenyl]-*N*-1,3,4-thiadiazol-2-yl-5*H*-[1]benzopyrano[2,3-*b*]pyridin-5-acetamide 41. **41** was prepared from **29a** according to method D. ^{1}H NMR (400 MHz, $CDCl_3$) δ 8.90 (s, 1H), 8.12−8.04 (m, 2H), 7.72 (d, J = 7.9 Hz, 1H), 7.56−7.46 (m, 3H), 7.35−7.29 (m, 2H), 7.22 (d, J = 7.5 Hz, 1H), 7.10−7.02 (m, 1H), 4.76 (s, 1H), 3.95−3.40 (m, 8H), 1.27 (d, J = 5.7 Hz, 6H). ESI-MS m/z 542.14 ($[M + H]^+$). HPLC t_R = 3.03 min.

[(5*S*)-2-[3-Fluoro-4-(1-morpholinylcarbonyl)phenyl]-α,α-dimethyl-*N*-1,3,4-thiadiazol-2-yl-5*H*-[1]benzopyrano[2,3-*b*]-pyridin-5-acetamide 42. **42** was prepared from **29b** according to method D. ^{1}H NMR (400 MHz, $CDCl_3$) δ 8.89 (s, 1H), 7.93−7.82 (m, 2H), 7.70 (d, J = 8.1 Hz, 1H), 7.60−7.49 (m, 2H), 7.42−7.30 (m, 2H), 7.19−7.07 (m, 2H), 4.55 (s, 1H), 3.95−3.66 (m, 6H), 3.43 (br s, 2H), 1.28 (d, J = 11.2 Hz, 6H). ESI-MS m/z 560.30 ($[M + H]^+$). HPLC t_R = 3.27 min.

[(5*S*)-2-[3-Fluoro-4-(1-pyrrolidinylcarbonyl)phenyl]-α,α-dimethyl-*N*-1,3,4-thiadiazol-2-yl-5*H*-[1]benzopyrano[2,3-*b*]-pyridin-5-acetamide 43. **43** was prepared from **29b** according to method D. ^{1}H NMR (400 MHz, $CDCl_3$) δ 8.93 (s, 1H), 7.85 (d, J = 9.6 Hz, 2H), 7.78 (d, J = 8.1 Hz, 1H), 7.58−7.49 (m, 2H), 7.32 (d, J = 3.5 Hz, 2H), 7.24 (d, J = 7.6 Hz, 1H), 7.12−7.03 (m, 1H), 4.83 (s, 1H), 3.70 (t, J = 6.9 Hz, 2H), 3.37 (t, J = 6.7 Hz, 2H), 2.09−1.87 (m, 4H), 1.29 (d, J = 11.1 Hz, 6H). ESI-MS m/z 544.25 ($[M + H]^+$). HPLC t_R = 3.44 min.

[(5*S*)-2-[4-(3,3-Difluoro-1-pyrrolidinylcarbonyl)-3-fluoro-phenyl]-α,α-dimethyl-*N*-1,3,4-thiadiazol-2-yl-5*H*-[1]benzo-pyrano[2,3-*b*]pyridin-5-acetamide 44. **44** was prepared from **29b** according to method D. ^{1}H NMR (400 MHz, $CDCl_3$) δ 8.91 (s, 1H), 7.87 (d, J = 9.1 Hz, 2H), 7.75 (dd, J = 7.8, 2.8 Hz, 1H), 7.60−7.46 (m, 2H), 7.34 (d, J = 3.5 Hz, 2H), 7.23 (d, J = 7.8 Hz, 1H), 7.12−7.03 (m, 1H), 4.77 (s, 1H), 4.09−3.89 (m, 2H), 3.80−3.59 (m, 2H), 2.57−2.33 (m, 2H), 1.28 (s, 6H). ESI-MS m/z 580.25 ($[M + H]^+$). HPLC t_R = 3.51 min.

[(5*S*)-2-[4-(3,3-Difluoro-1-pyrrolidinylcarbonyl)-3-chloro-phenyl]-α,α-dimethyl-*N*-1,3,4-thiadiazol-2-yl-5*H*-[1]benzo-pyrano[2,3-*b*]pyridin-5-acetamide 45. **45** was prepared from **29c** according to method D. ^{1}H NMR (400 MHz, $CDCl_3$) δ 8.91 (s, 1H), 8.18−8.12 (m, 1H), 7.98 (dt, J = 8.1, 1.6 Hz, 1H), 7.76 (dd, J = 7.8, 2.8 Hz, 1H), 7.50 (dd, J = 7.7, 1.9 Hz, 1H), 7.43 (dd, J = 7.9, 1.9 Hz, 1H), 7.37−7.31 (m, 2H), 7.24 (d, J = 8.6 Hz, 1H), 7.08 (ddd, J = 8.2, 5.2, 2.8 Hz, 1H), 4.79 (s, 1H), 4.10−3.89 (m, 2H), 3.67−3.46 (m, 2H), 2.56−2.34 (m, 2H), 1.28 (br s, 6H). ESI-MS m/z 596.29 ($[M + H]^+$). HPLC t_R = 3.57 min.

1,1,1-Trifluoromethanesulfonic Acid 9-[1,1-Dimethyl-2-oxo-2-(1,3,4-thiadiazole-2-ylamino)ethyl]-9*H*-xanthen-3-yl Ester (47). To a solution of (*S*)-2-(3-hydroxy-9*H*-xanthen-9-yl)-2-methyl-*N*-(1,3,4-thiadiazol-2-yl)propanamide **46** (200 mg, 0.545 mmol) in dichloromethane (5 mL) at 0 °C under nitrogen was added triethylamine (0.182 mL, 1.31 mmol) followed by 1,1,1-trifluoro-*N*-phenyl-*N*-(trifluoromethylsulfonyl)methanesulfonamide (292 mg, 0.817 mmol). The reaction mixture was allowed to stir at 0 °C for 2.5 h, then partitioned between dichloromethane and saturated aqueous $NaHCO_3$ solution. The organic layer was dried over Na_2SO_4 and concentrated. Purification by flash column chromatography (40 g silica, 50% ethyl acetate in hexanes) afforded the product **47** (150 mg, 55% yield) as a white solid. ESI-MS m/z 500.29 ($[M + H]^+$). HPLC t_R = 3.99 min.

6-[9-[1,1-Dimethyl-2-oxo-2-(1,3,4-thiadiazol-2-ylamino)ethyl]-9*H*-xanthen-3-yl-*N*,*N*-dimethyl-3-phenylcarboxamide 48. To a solution of triflate **47** (20 mg, 0.06 mmol) in DMF (1 mL) in a microwave vessel was added 4-[*N*,*N*-dimethylaminocarbonyl]phenylboronic acid (23 mg, 0.12 mmol), followed by aqueous potassium phosphate (2.0 M, 0.1 mL) and tetrakis(triphenylphophine)palladium(0) (10 mg, 0.009 mmol). A stream of nitrogen gas was bubbled through the mixture for 15 min, which was then microwaved at 120 °C for 30 min. The reaction mixture was purified by preparative HPLC to give the desired product **48** (8.95 mg, 30% yield) as a white solid. ^{1}H NMR (400 MHz, CDCl3) δ 8.89 (br s, 1H), 7.63 (d, J = 7.6 Hz, 2H), 7.52 (d, J = 7.6 Hz, 2H), 7.41 (s, 1H), 7.34−7.26 (m, 2H), 7.24 (br s, 1H), 7.19 (d, J = 8.1 Hz, 2H), 7.08−6.98 (m, 1H), 4.57 (s, 1H), 3.17 (br s, 3H), 3.07 (br s, 3H), 1.25 (br s, 6H). ESI-MS m/z 499.12 ($[M + H]^+$). HPLC t_R = 3.61 min.

(9*S*)-α,α-Dimethyl-3-(4,4,5,5-tetramethyl-1,3,2-dioxaborolan-2-yl)-*N*-1,3,4-thiadiazol-2-yl-9*H*-xanthene-9-acetamide (49). To a solution of the triflate **47** (160 mg, 0.32 mmol) in 1,4-dioxane (3 mL) were sequentially added 1,1′-bis(diphenylphosphino)ferrocenepalladium(II) dichloride−dichloromethane complex (24 mg, 0.03 mmol), bis(pinacolato)diboron (120 mg, 0.47 mmol), and potassium acetate (96 mg, 0.98 mmol). A stream of nitrogen gas was blown through the reaction mixture for 15 min, which was then heated at 80 °C for 5 h. The reaction mixture was concentrated in vacuo, and the residue was purified by flash column chromatography (12 g silica, 20−50% ethyl acetate in hexanes) to provide the product **49** (120 mg, 79% yield) as a yellow oil. ESI-MS m/z 478.08 ($[M + H]^+$). HPLC t_R = 4.07 min.

6-[9-[1,1-Dimethyl-2-oxo-2-(1,3,4-thiadiazol-2-ylamino)-ethyl]-9*H*-xanthen-3-yl-*N*,*N*-dimethyl-3-pyridinecarboxamide 52. *a.* To a solution of 6-chloronicotinic acid (7.4 mg, 0.047 mmol) in DMF (1 mL) was added the borolate **49** (15 mg, 0.031 mmol), followed by aqueous potassium phosphate (2.0 M, 0.1 mL) and tetrakis-(triphenylphophine)palladium(0) (10 mg, 0.009 mmol). A stream of nitrogen gas was bubbled through the mixture for 15 min, which was then heated at 100 °C for 2 h. The reaction mixture was purified by preparative HPLC to give the acid intermediate **50** as a TFA salt which was lyophilized from acetonitrile/water to give a white powder (3.1 mg, 21% yield). ESI-MS m/z 473.11 ($[M + H]^+$). HPLC t_R = 3.55 min.

b. A mixture of the acid **50** (10 mg, 0.021 mmol), HOBT monohydrate (4.3 mg, 0.032 mmol), EDCI (6.12 mg, 0.032 mmol), triethylamine (0.1 mL), and dimethylamine hydrochloride (3.43 mg, 0.042 mmol) in acetonitrile (1 mL) was heated at 80 °C for 12 h. The reaction mixture was then purified by preparative HPLC to give the final product **52**, which was lyophilized from acetonitrile/water to give a white powder (4 mg, 38% yield). ^{1}H NMR (400 MHz, $CDCl_3$) δ 8.95−8.84 (m, 2H), 8.08 (s, 1H), 7.87 (d, J = 8.1 Hz, 1H), 7.73 (d, J = 1.0 Hz, 1H), 7.63 (d, J = 7.6 Hz, 1H), 7.33−7.28 (m, 2H), 7.21−7.13 (m, 2H), 7.08−7.02 (m, 1H), 4.52 (s, 1H), 3.19 (s, 3H), 3.12 (s, 3H), 1.25 (s, 6H). ESI-MS m/z 500.20 ($[M + H]^+$). HPLC t_R = 3.26 min.

6-[9-[1,1-Dimethyl-2-oxo-2-(1,3,4-thiadiazol-2-ylamino)-ethyl]-9*H*-xanthen-3-yl-*N*,*N*-dimethyl-3-pyrimidinecarboxamide 53. The procedure for preparing **52** was followed. The desired product **53** was obtained in two steps with 15% overall yield from the borolate **49**. ^{1}H NMR (400 MHz, $CDCl_3$) δ 8.93−8.83 (m, 3H), 8.28 (d, J = 1.5 Hz, 1H), 8.11 (dd, J = 8.1, 1.5 Hz, 1H), 7.30 (d, J = 8.1 Hz, 2H), 7.23−7.13 (m, 2H), 7.07−6.97 (m, 1H), 4.57 (s, 1H), 3.22−3.09 (m, 6H), 1.24 (d, J = 5.6 Hz, 6H). ESI-MS m/z 501.05 ($[M + H]^+$). HPLC t_R = 3.42 min.

Nuclear Receptor Binding Assays. The GR ligand binding assay was conducted in fluorescence polarization format which measures the competition between a test compound and a fluorescently labeled ligand (GS-red) for binding to the full length or ligand binding domain of GRα (Invitrogen, catalog no. P2893). Compounds were tested in concentrations ranging from 5 μM to 85 pM. IC_{50} values were determined by fitting the fluorescence polarization signal data using a four-parameter logistic equation. The K_i values were determined by application of the Cheng−Prusoff equation to the IC_{50} values, where $K_i = IC_{50}/(1 + \text{ligand concentration}/K_d)$ (Cheng, Y.; Prusoff, W. H. *Biochem. Pharmacol.*

1973, *22*, 3099−3108). The K_d used for GR was 0.3 nM as supplied by the assay manufacturer (Invitrogen, catalog no. P2893). Data shown represent the mean values of two or more experiments.

PR, ER, and AR ligand binding assays were also conducted in fluorescence polarization format which measures the competition between a test compound and a fluorescently labeled ligand for binding to the full length or ligand binding domain of the nuclear hormone receptor.

Transrepression Assays. AP-1 activity is measured using an AP-1 response element (five copies) cloned into a luciferase reporter vector. This reporter is stably transfected into the human A549 lung epithelial cell line. AP-1 activity is induced by addition of phorbol myristate acetate (PMA) (15 ng/mL), and inhibition of induction by compounds is quantitated by measuring decreased luciferase activity. NFκB is measured using a truncated, NFκB dependent E-selectin promoter (−383 bp from transcriptional start) cloned into a luciferase reporter vector. This reporter is stably transfected into the human A549 lung epithelial cell line. NFκB activity is induced using IL-1β (0.5 ng/mL), and inhibition of induction by compounds is quantitated by measuring decreased luciferase activity.

Transactivation Assays. *a. GAL4DBD-GR(LBD) Reporter Assay.* The direct transcriptional activity is measured using a chimera between the GAL4 DNA-binding domain and the human GR ligand-binding domain (GR-LBD) cloned into a GAL4 Luciferase reporter system. This reporter system is stably transfected into a NP-1 HeLa cell line (Webster, N. J. G.; Green, S.; Jin, J. R.; Chambon, P. *Cell* **1988**, *54* (2), 199−207). The hormone-binding domains of the glucocorticoid receptor contains an inducible transcription activation function. Response to ligand/compound induced binding is quantitated by measuring luciferase activity. Direct activation of the GR-LBD by compounds (agonist) can be measured as increased luciferase activity after a 20 h of incubation at 37 °C/5% CO_2.

b. GAL4 DBD-GR(LBD) Reporter Assay (Antagonist Mode). The antagonist mode is the same as the agonist mode except that 100 nM dexamethasone is added with test compound.

c. TAT Induction Assay. Enzymatic assay[18] was used to measure the induction of tyrosine aminotransferase activity in cultured hepatoma cell line (human 13D3/Huh7). Briefly, on day 1, hepatoma cells (3D3/Huh, plate 20K cells/well) were plated in a 96-well flat-bottom tissue-culture-treated plate and incubated overnight at 37 °C/5% CO_2. On day 2, the growth medium was removed from the wells and replaced with assay medium containing 20 μM forskolin and test compounds, which was then incubated overnight at 37 °C with 5% CO_2. On day 3, the assay medium was removed and 100 μL/well of lysis buffer (125 mM potassium phosphate buffer, pH 7.6, 140 mM KCl, 1 mM EDTA, and 0.1% NP-40) was added. The lysates were assayed for TAT activity. In a new 96-well plate, 136 μL/well TAT substrate (200 mM potassium phosphate buffer, pH 7.6, 5.4 nM tyrosine sodium salt, 0.06 mM pyridoxal 5′-phosphate, and 10.8 mM α-ketoglutarate) and 50 μL/well lysate were added and mixed. The plates were incubated at 37 °C for 4 h. The TAT enzymatic reaction was stopped with KOH and incubated for an additional 30 min at 37 °C. The absorbance was measured at 340 nm. Results were expressed as percent activation, and EC_{50} values were calculated.

d. Glutamine Synthetase (GS) Induction Assay. An enzymatic assay was used to measure the induction of GS activity in the human osteosarcoma cell line MG-63. The cell line was maintained in log phase in growth medium (Dulbecco's modified Eagle's medium [DMEM, Invitrogen] with 10% charcoal−dextran treated fetal calf serum [FCS, Hyclone], penicillin/streptomycin [10 000 U/mL and 10 mg/mL, respectively], and 2 mM L-glutamine). Briefly, on day 1 MG-63 cells were plated in assay medium (growth medium but without phenol red and L-glutamine) at a density of 50 000 cells/well (200 μL/well) in 96-well flat-bottom tissue-culture-treated plates and incubated overnight at 37 °C with 5% CO_2. On day 2, the assay medium was removed from the wells and replaced with 100 μL/well induction medium (DMEM without L-glutamine, 1% FCS, and penicillin/streptomycin) and test compounds followed by incubation overnight at 37 °C with 5% CO_2. On day 3, the induction medium was removed and the wells were washed three times with 200 μL/well PBS. After the last wash, PBS was removed and the cells were lysed at room temperature with 30 μL of 50 mM imidazole (pH 6.8)/0.1% Trixon-100 per well. Then 30 μL of GS assay mix (imidazole, 50 mM; arsenic acid, 25 mM; ADP, 0.16 mM; L-glutamine, 50 mM; $MnCl_2$, 2 mM; hydroxylamine, 25 mM) was added per well, and the plates were incubated at 37 °C, 5% CO_2 for 90 min. At the end of the incubation period, 120 μL of ferric chloride stop solution (ferric chloride, 2.42%; TCA, 1.45%; HCl, 1.82%) was added per well, and the absorption was read at 540 nm.

e. Alkaline Phosphatase Induction Assay. An enzymatic assay was used to measure the induction of alkaline phosphatase activity in the human osteosarcoma cell line SAOS-2. The cell line was maintained in log phase in growth medium (McCoy's 5A [Invitrogen] with 15% fetal bovine serum [FBS, Summit] and penicillin/streptomycin [10 000 U/mL and 10 mg/mL, respectively]). Briefly, on day 1 SAOS-2 cells were plated in assay medium (growth medium except using 15% charcoal−dextran treated fetal calf serum [FCS, Hyclone]) at a density of 3000 cells/well (100 μL/well) in 96-well flat-bottom tissue-culture-treated plates and incubated overnight at 37 °C with 5% CO_2. On day 2, the assay medium was removed from the wells and replaced with 200 μL/well induction medium (assay medium except using 1.5% charcoal−dextran treated FCS) and test compounds followed by incubation for 3 days at 37 °C with 5% CO_2. After the third day of compound treatment, the induction medium was removed and the wells were washed three times with 200 μL/well cold PBS. After the last wash, PBS was removed and the cells were lysed at room temperature with 100 μL per well of 12.5 mM $NaHCO_3$, 12.5 mM Tris, 0.01% sodium azide, and 0.05% Triton X-100. Then 25 μL of cell lysate was added to 100 μL of alkaline phosphatase assay mix (*p*-NPP diluted in 1× KPL DEA substrate buffer to 3 mg/mL) and the plates were incubated in the dark at room temperature for 15 min. At the end of the incubation period, 100 μL per well of 1 N HCL stop solution was added per well, and the absorbance was read at 405 nm.

f. Human Whole Blood Assays for TNFα and IL-1β. Human whole blood (two donors per experiment) was drawn into syringes containing ACD-A and kept at room temperature until initiation of the experiment (about 1 h). The blood was plated into 96-well flat-bottom, polystyrene, tissue-culture-treated plates (BD Falcon) at 180 μL/well. An amount of 10 μL of 20× test compound dilutions was added per well, mixed, and the plates were incubated overnight (about 20 h) at 37 °C with 5% CO_2. The next day, 10 μL of 20× LPS (Sigma-Aldrich *E. coli* 055/B5 LPS; for TNFα induction, final concentration of LPS was 100 ng/mL) or 20× human recombinant IL-1β (R & D Systems; for IL-8 induction, final concentration of IL-1β was 10 ng/mL) was added per well. The plates were incubated for an additional 5 h, centrifuged at low speed, and the plasmas were harvested for immediate analysis by ELISA or were frozen at −20 °C. TNFα and IL-8 induction was quantitated by ELISA (R & D Systems).

Carageenan Paw Edema (CPE) Assay. Male Sprague−Dawley rats were isolated and fasted overnight and up to an additional 6 h on the day of the study. Baseline paw volume measurements were obtained by immersing each hind paw to the level of the hair-line in a water-based plethysmometer. Rats were administered a single oral dose of test compound(s) in biologically acceptable medium. Two hours after dosing, while under anesthesia, both hind paws were injected subcutaneously with 1% carrageenan in PBS. Paw volume measurements were obtained 4 h after challenge. Paw swelling was calculated by subtracting the baseline values from the postchallenge measurements.

Adjuvant-Induced Arthritis. Male Lewis rats were injected intradermally at the shaved based of the tail on day 0 with 100 μL of

10 mg/mL freshly ground *Mycobacterium butyricum* in incomplete Freund's adjuvant, then randomized into dose groups (n = 8/group). Test compounds were dosed po in solution (EtOH/TPGS/PEG300, 5:5:90) once daily. Baseline paw measurements were taken between days 7 and 10, and measurements were taken three times per week after disease develops (between days 11 and 14).

■ ASSOCIATED CONTENT

Supporting Information. Spectral data for key compounds **35** and **37** and X-ray crystal structure of (*R*)-(+)-α-methylbenzylamine salt of **12b**. This material is available free of charge via the Internet at http://pubs.acs.org.

■ AUTHOR INFORMATION

Corresponding Author

*Phone: 609-252-3060. Fax: 609-252-6804. E-mail: David.Weinstein@bms.com.

■ ACKNOWLEDGMENT

The authors are grateful to the following colleagues for their support of the project and their help in the preparation of this manuscript: Katy Van Kirk, Cullen Cavallaro, Dauh-Rurng Wu, Leslie Leith, Mary Ellen Cvijic, Melissa Yarde, Ding Ren Shen, Jun Dai, Mary Malley, Michael Galella, Sarah Traeger, Bingwei Yang, and Jim Sheppeck.

■ DEDICATION

†Dedicated to Professor K. C. Nicolaou on the occasion of his 65th birthday.

■ ABBREVIATIONS USED

ADME, absorption, distribution, metabolism, excretion; ALP, alkaline phosphatase; AR, androgen receptor; AP-1, activator protein 1; CPE, carrageenan-induced paw edema; DAC, deacylcortivazol; dex, dexamethasone; dppf, 1,1′-bis(diphenylphosphino)-ferrocene; EDC, 1-ethyl-3-(3-dimethylaminopropyl)carbodiimide; ER, estrogen receptor; GS, glutamine synthetase; GR, glucocorticoid receptor; HATU, (2-(7-aza-1*H*-benzotriazole-1-yl)-1,1,3,-3-tetramethyluronium hexafluorophosphate); HOBT, hydroxybenzotriazole; IL, interleukin; LPS, lipopolysaccharide; mCPBA, *m*-chloroperbenzoic acid; MR, mineralocorticoid receptor; NFκB, nuclear factor kappa B; PAMPA, parallel artificial membrane permeability assay; PR, progesterone receptor; pred, prednisolone; SFC, supercritical fluid chromatography; TA, transactivation; TAT, tyrosine amino transferase; TNFα, tumor necrosis factor α; TR, transrepression

■ REFERENCES

(1) Goulding, N. J.; Flower, R. J., Ed. *Glucocorticoids*; Birkhäuser Verlag: Basel, Switzerland, 2001.

(2) Buttgereit, F.; Burmester, G.-R.; Lipworth, B. J. Optimised glucocorticoid therapy: the sharpening of an old spear. *Lancet* **2005**, *365*, 801–806.

(3) For recent reviews of glucocorticoid receptor modulators, see the following: (a) Berlin, M. Recent advances in the development of novel glucocorticoid receptor modulators. *Expert Opin. Ther. Pat.* **2010**, *20*, 855–873. (b) Hudson, A. R.; Roach, S. L.; Higuchi, R. I. Recent developments in the discovery of selective glucocorticoid receptor modulators (SGRMs). *Curr. Top. Med. Chem.* **2008**, *8*, 750–765. (c) Takahashi, H.; Razavi, H.; Thomson, D. Recent progress in the discovery of novel glucocorticoid receptor modulators. *Curr. Top. Med. Chem.* **2008**, *8*, 521–530. (d) Schäcke, H.; Berger, M.; Hansson, T. G.; McKerrecher, D.; Rehwinkel, H. *Expert Opin. Ther. Pat.* **2008**, *18*, 339.(e) Regan, J.; Razavi, H.; Thomson, D. Advances toward Dissociated Non-steroidal Glucocorticoid Receptor Agonists. In *Annual Reports in Medicinal Chemistry*; Elsevier: New York, 2008; Vol. 43, Chapter 9, pp 141− 154. For a very recent disclosure, see the following: (f) Riether, D.; Harcken, C.; Razavi, H.; Kuzmich, D.; Gilmore, T.; Bentzien, J.; Pack, E. J., Jr.; Souza, D.; Nelson, R. M.; Kukulka, A.; Fadra, T. N.; Zuvela-Jelaska, L.; Pelletier, J.; Dinallo, R.; Panzenbeck, M.; Torcellini, C.; Nabozny, G. H.; Thomson, D. S. Nonsteroidal dissociated glucocorticoid agonists containing azaindoles as steroid A-ring mimetics. *J. Med. Chem.* **2010**, *53*, 6681–6698.

(4) (a) Newton, R.; Holden, N. S. Separating transrepression and transactivation: a distressing divorce for the glucocorticoid receptor? *Mol. Pharmacol.* **2007**, *72*, 799–809. (b) Clark, A. R. Anti-inflammatory functions of glucocorticoid-induced genes. *Mol. Cell. Endocrinol.* **2007**, *275*, 79–97. (c) Beck, I. M. E.; Berghe, W. V.; Vermeulen, L.; Yamamoto, K. R.; Haegeman, G.; De Bosscher, K. Crosstalk in inflammation: the interplay of glucocorticoid receptor-based mechanisms and kinases and phosphatases. *Endocr. Rev.* **2009**, *30*, 830–882.

(5) Yang, B. V.; Vaccaro, W.; Doweyko, A. M.; Doweyko, L. M.; Huynh, T.; Tortolani, D.; Nadler, S. G.; McKay, L.; Somerville, J.; Holloway, D. A.; Habte, S.; Weinstein, D. S.; Barrish, J. C. Discovery of novel dihyro-9,10-ethano-anthracene carboxamides as glucocorticoid receptor modulators. *Bioorg. Med. Chem. Lett.* **2009**, *19*, 2139–2143.

(6) Yang, B. V.; Weinstein, D. S.; Doweyko, L. M.; Gong, H.; Vaccaro, W.; Huynh, T.; Xiao, H.; Doweyko, A. M.; McKay, L.; Holloway, D. A.; Somerville, J. E.; Habte, S.; Cunningham, M.; McMahon, M.; Townsend, R.; Shuster, D.; Dodd, J. H.; Nadler, S. G.; Barrish, J. C. Dimethyl-diphenyl-propanamide derivatives as non-steroidal dissociated glucocorticoid receptor agonists. *J. Med. Chem.* **2010**, *53*, 8241–8251.

(7) (a) Wang, Y.; Zhong, D.; Chen, X.; Zheng, J. Identification of quinone methide metabolites of dauricine in human liver microsomes and rat bile. *Chem. Res. Toxicol.* **2009**, *22*, 824–834. (b) Monks, T. J.; Jones, D. C. The metabolism and toxicity of quinines, quinonimines, quinine methods, and quinine-thioethers. *Curr. Drug Metab.* **2002**, *3*, 425–438.

(8) Bledsoe, R. K.; Montana, V. G.; Stanley, T. B.; Thomas, B.; Delves, C. J.; Apolito, C. J.; McKee, D. D.; Consler, T. G.; Parks, D. J.; Stewart, E. L.; Willson, T. M.; Lambert, M. H.; Moore, J. T.; Pearce, K. H.; Xu, H. E. Crystal structure of the glucocorticoid receptor ligand binding domain reveals a novel mode of receptor dimerization and coactivator recognition. *Cell* **2002**, *110*, 93–105.

(9) Suino-Powell, K.; Xu, Y.; Zhang, C.; Tao, Y.-G.; Tolbert, W. D.; Simons, S. S.; Xu, H. E. Doubling the size of the glucocorticoid receptor ligand binding pocket by deacylcortivazol. *Mol. Cell. Biol.* **2008**, *28*, 1915–1923.

(10) Biggadike, K.; Bledsoe, R. K.; Coe, D. M.; Cooper, T. W. J.; House, D.; Iannone, M. A.; Macdonald, S. J. F.; Madauss, K. P.; McLay, I. M.; Shipley, T. J.; Taylor, S. J.; Tran, T. B.; Uings, I. J.; Weller, V.; Williams, S. P. Design and X-ray crystal structures of high-potency nonsteroidal glucocorticoid agonists exploiting a novel binding site on the receptor. *Proc. Natl. Acad. Sci. U.S.A.* **2009**, *106*, 18114–18119.

(11) Doweyko, A. M. Steroid nuclear hormone receptors: the allosteric conversation. *Drug Dev. Res.* **2007**, *68*, 95–106.

(12) (a) Paliogianni, F.; Boumpas, D. T. In *Glucocorticoids*; Goulding, N. J.; Flower, R. J., Eds.; Birkhauser Verlag: Basel, Switzerland, 2001; pp 81− 101. (b) Rhen, T.; Cidlowski, J. A. Antiinflammatory action of glucocorticoids−new mechanisms for old drugs. *N. Engl. J. Med.* **2005**, *353*, 1711–1723. (c) Brattsand, R.; Linden, M. Cytokine modulation by glucocorticoids: mechanisms and actions in cellular studies. *Aliment. Pharmacol. Ther.* **1996**, *10* (Suppl. 2), 81–90.

(13) Sabokbar, A.; Millett, P. J.; Myer, B.; Rushton, N. A rapid, quantitative assay for measuring alkaline phsophatase activity in osteoblastic cells in vitro. *Bone Miner.* **1994**, *27*, 57–67.

(14) (a) Santoro, J. C.; Harris, G.; Sitlani, A. Colorimetric detection of glutamine synthetase-catalyzed transferase activity in glucocorticoid-treated skeletal muscle cells. *Anal. Biochem.* **2001**, *289*, 18–25. (b) Minet, R.; Villie, F.; Marcollet, M.; Meynial-Denis, D.; Cynober, L. Measurement of glutamine synthetase activity in rat muscle by a colorimetric assay. *Clin. Chim. Acta* **1997**, *268*, 121–132.

(15) Schäcke, H.; Döcke, W.-D.; Asadullah, K. Mechanisms involved in the side effects of glucocorticoids. *Pharmacol. Ther.* **2002**, 23–43.

(16) (a) Nicolaides, N. C.; Galata, Z.; Kino, T.; Chrousos, G. P.; Charmandari, E. The human glucocorticoid receptor: molecular basis of biologic function. *Steroids* **2010**, *75*, 1–12. (b) Haller, J.; Mikics, E.; Makara, G. B. The effects of non-genomic glucocorticoid mechanisms on bodily functions and the central nervous system. A critical review of findings. *Front. Neuroendocrinol.* **2008**, *29*, 273–291. (c) Newton, R.; Leigh, R.; Giembycz, M. A. Pharmacological strategies for improving the efficacy and therapeutic ratio of glucocorticoids in inflammatory lung diseases. *Pharmacol. Ther.* **2010**, *125*, 283–327. (c) Goulding, N. J. The molecular complexity of glucocorticoid actions in inflammation—a four-ring circus. *Curr. Opin. Pharmacol.* **2004**, *4*, 629–666. (d) Chrousos, G. P.; Kino, T. Intracellular glucocorticoid signaling: a formerly simple system turns stochastic. *Sci. STKE* **2005**, *304*, pe48.

(17) Wang, J. C.; Shah, N.; Pantoja, C.; Meijsing, S. H.; Ho, J. D.; Scanlan, T. S.; Yamamoto, K. R. Novel arylpyrazole compounds selectively modulate glucocorticoid receptor regulatory activity. *Genes Dev.* **2006**, *20*, 689–699.

(18) Assay was developed as a modification of the method of Granner and Tomkins (Granner, D. K.; Tomkins, G. M. *Methods Enzymol.* **1970**, 633−637) and Diamondstone (Diamondstone, T. I. *Anal. Biochem.* **1966**, *16*, 395−401).